8 Long-term development directions of PVD/CVD coatings deposited onto sintered tool materials

A.D. Dobrzańska-Danikiewicz*, K. Gołombek,
D. Pakuła, J. Mikuła, M. Staszuk, L.W. Żukowska
Faculty of Mechanical Engineering, Silesian University of Technology,
ul. Konarskiego 18a, 44-100 Gliwice, Poland
* Corresponding author: E-mail address: anna.dobrzanska-danikiewicz@polsl.pl

Abstract

Purpose: *The purpose of this chapter is to evaluate strategic development perspectives of physical/ chemical vapour deposition of monolayer, multilayer and gradient coatings onto sintered tool materials with cemented carbides, cermets and tool ceramics substrates. The coating type was adopted as the criterion for technology division, thus obtaining eight technology groups for carried out research.*

Design/methodology/approach: *In the framework of foresight-materials science research: a group of matrices characterising technology strategic position was created, materials science experiments using high-class specialised equipment were conducted and technology roadmaps were prepared.*

Findings: *High potential and attractiveness were shown of the analysed technologies against the environment, as well as a promising improvement of mechanical and functional properties as a result of covering with the PVD/CVD coatings.*

Research limitations/implications: *Research pertaining to covering sintered tool materials with the PVD/CVD coatings is part of a bigger research project aimed at selecting, researching and characterizing priority innovative material surface engineering technologies.*

Practical implications *The presented results of experimental materials science research prove the significant positive impact of covering with the PVD/CVD coatings on the structure and mechanical properties of sintered tool materials, which leads to the justification of their including into the set of priority innovative technologies recommended for application in industrial practice.*

Originality/value: *The advantage of the chapter are results of comparative analysis of sintered tools materials with different types of coatings deposited in the PVD/CVD processes together with the recommended strategies of conduct, strategic development tracks and roadmaps of these technologies.*

Keywords: *Manufacturing and processing; Thin and thick coatings; Sintered tool materials; Foresight; Technology Roadmapping*

This chapter has been also published as:

A.D. Dobrzańska-Danikiewicz, K. Gołombek, D. Pakuła, J. Mikuła, M. Staszuk, L.W. Żukowska, Long-term development directions of PVD/CVD coatings deposited onto sintered tool materials, Archives of Materials Science and Engineering 49/2 (2011) 69-96.

1. Introduction

A recently announced "Europe 2020" strategy replacing the current Lisbon Strategy envisages comprehensive actions at a European, national and regional level aiming to support a more effective, competitive and low-emission economy based on knowledge and innovation ensuring high employment and social and territorial cohesion. One of the five strategic goals of the contemporary Europe in the field of economy provides for the growing level of R&D and innovation investments. 3% of the EU's GDP will be spent in total for this purpose until 2020 from public and private funds. For the economic and social effects achieved to be satisfactory and as expected, the above financial resources have to be invested properly in the fields of science and industries generating the highest added value in the future. The above reasons have been decisive in the last decade for widespread interest in foresight research, also in respect of material engineering, being the subject of numerous projects implemented and currently held globally [1-3] and in Poland [4-8]. An analysis of such projects' outcomes and scope combined with literature review [9] and the observation of development trends in the industry indicating the sharp growth of materials surface engineering in many technically advanced countries, set a basis for conducting extensive research aimed at identifying the priority, innovative technologies and strategic directions of development in this field [10]. The relevance and adequacy of the assessments is ensured by the synergic interaction of materials science

research and foresight methods. The foresight-material science research has been carried out using the custom methodology [11] of the Computer Aided Foresight Integrated Research that organises, stream¬lines and modernises the actual process of foresight research by applying information technology [12] encompassing: a virtual organisation, web platform and neural networks. The following technologies have been investigated to date: laser treatment of hot-work steels [13], casting magnesium alloys [14] and polycrystalline silicon used for photovoltaic purposes [15]; deposition of PVD and CVD coatings, including nanostructural coatings onto a brass substrate [16]; surface manufacture of graded and composite materials including nanostructural materials with the required soft and hard magnetic properties [17] and selected methods of steel thermochemical treatment [18]. The group of high-potential technologies include also PVD and CVD with a broad spectrum of current and future applications, notably in the tool industry, especially for cutting processes.

Efforts to enhance the life of cutting tools on one hand preconditions a constant search for new materials with improved properties characteristic for i.e. sintered tool materials [19-26], on the other hand contributes to increased interest in modern PVD/ CVD coatings. World and domestic papers review shows that deposited coatings contribute to improving strength [27-30], tribological [31-37] and anti-corrosive [38-43] properties as well as higher resistance to wear [44-56] and high temperature [57-61]. A beneficial combination: a substrate - a thin PVD/CVD coating allows to achieve the unique properties of cutting tools, i.e. made of high-speed steels [62-68]. Thin coatings produced from a gaseous phase formed as a result of chemical reactions occurring in a hot substrate [69] enable to produce dense and pure layers, using materials featuring low diffusion coefficients on different substrates, also those with a complex geometry [9,70]. The nanocrystalline [71-73] and graded [70,74-78] coatings deposited in PVD processes occupy a special place amid the coatings discussed. A tool material deposited with a graded coating features a lower friction co-efficient, higher microhardness, resistance to adherence and diffusion wear and to oxidisation. This inclines to analyse such groups of technologies both, in the technical and economic context, hence requires that their long-term development prospects need to be evaluated.

The purpose of this study is a comparative analysis of various, selected technologies of physical and chemical vapour deposition differing in the type of the deposited coatings. The subject of the comparative analysis are the results of investigations into the structure and properties of sintered tool materials with the PVD/CVD coatings applied as well as the value of the individual technologies against the environment and their long-term development prospects

with the recommended action strategies and the forecast multi-variant development tracks determined through expert research. The final research results show the strategic position of the analysed technologies against the surface engineering background as well as are a compact compendium of knowledge presented using technology roadmaps and technology information sheets.

2. Interdisciplinary research approach

The research efforts concerning the selected physical and chemical vapour deposition technologies differing in the type of a substrate and chemical composition, as well as the type and number of the layers of the coating deposited are of an interdisciplinary character. The foresight-materials science research method employed origins directly from organisation and management (technology foresight) as well as material engineering (surface engineering). A much broader insight into the concept was, however, required at some stages of the research, hence the following areas of detailed knowledge were also used: computer science embracing: information technology and artificial intelligence (neural networks, Monte Carlo methods); statistics; econometrics; operational studies; construction and operation of machinery; automation and robotisation of industrial processes; strategic, tactical and operation management; quality and environment management; accounting and finance.

The research has been carried out using sintered tool materials based on cemented carbides: (A) WC, Co, (B) WC, TiC, TaC, Co, cermets: (A) Ti(C,N), WC, TiC, TaC, Co, Ni, (B) Ti(C,N), TiC, TaC, WC, Co, Ni, oxide and nitride ceramics and sialon ceramics deposited in PVD and CVD processes with a wide range of monolayer, multilayer, graded coatings resistant to wear. The following eight homogenous groups have been distinguished between from the physical and chemical vapour deposition technologies on sintered tool materials for the purpose of foresight and materials science works carried out under this study by adopting the type of coatings deposited as a criterion of grouping:

(K) The physical vapour deposition of the simple monolayer coatings,
(L) The physical vapour deposition of the complex, classical monolayer coatings,
(M) The physical vapour deposition of the complex, nanocrystalline monolayer coatings,
(N) The physical vapour deposition of the multilayer coatings, number of layers $n<10$,

Table 1. *Tested materials classification scheme*

Coating type			Coating composition	Process	Symbol	Substrate
monolayer	simple		TiN	PVD	(K)	Cemented carbides: A-type: WC, Co B-type: WC, TiC, TaC, Co Cermets: A-type: Ti(C,N), WC, TiC, TaC, Co, Ni B-type: Ti(C,N), TiC, TaC, WC, Co, Ni Al_2O_3+ZrO_2 oxide ceramics Al_2O_3+TiC oxide ceramics Al_2O_3+$SiC_{(w)}$ oxide ceramics Si_3N_4 nitride ceramics SiAlON
	complex	classical	Ti(C,N) (Ti,Al)N	PVD	(L)	
		nanocrystalline	(Ti,Al)N Ti(C,N)	PVD	(M)	
multilayer	*n**<10		TiN+TiC+TiN TiN+(Ti,Al,Si)N+TiN TiN+Al_2O_3 TiC+TiN Al_2O_3+TiN TiN+TiC/TiN Ti(C,N)+Al_2O_3+TiC Ti(C,N)+Al_2O_3+TiN Ti(C,N)+Al_2O_3+TiN TiN+Al_2O_3+TiN TiC+Ti(C,N)+Al_2O_3+TiN TiN+Al_2O_3+TiN+Al_2O_3+TiN	PVD	(N)	
				CVD	(O)	
	*n**≥10		TiN+multi(Ti,Al,Si)N+TiN multi(Al,Cr)N	PVD	(P)	
graded	step-graded		Ti(C,N)+ (Ti,Al)N TiN+(Ti,Al,Si)N+TiN TiN+(Ti,Al,Si)N+(Al,Si,Ti)N	PVD	(R)	
	continuous		Ti(B,N) Ti(C,N) (Ti,Zr)N (Al,Ti)N (Ti,Al)N	PVD	(S)	

* *n* – number of layers

(O) The chemical vapour deposition of the multilayer coatings, number of layers n<10,

(P) The physical vapour deposition of the multilayer coatings, number of layers n≥10,

(R) The physical vapour deposition of the step-graded coatings,

(S) The physical vapour deposition of continuous graded coatings.

A detailed overview and classification of tool materials with their coatings deposited in physical and chemical vapour deposition processes are presented in Table 1.

2.1. Materials science methodology

Surface topography and the structure of the coatings deposited was examined on the transverse fractures with a scanning electron microscope SUPRA 35 by Zeiss with the accelerating voltage of 5-20 kV. A side detector (SE) and InLens detector was used to produce structure images by using Secondary Electrons detection and Back Scattered Electrons detection. Notches were cut on the tested specimens with a diamond disc to obtain a brittle fracture on the tested specimens, and then they were broken and pre-cooled in liquid nitrogen.

The quantitative and qualitative analysis of the tested coatings' chemical composition was made with the EDS scattered X-ray radiation spectroscopy method using an EDS TRIDEX XM4 spectrometer by EDAX incorporated into an electron scanning microscope Zeiss Supra 35. The tests were performed with the accelerating voltage of 20 kV.

Diffraction investigations and the investigations of thin foil structures were performed with a JEM 3010 UHR transmission electron microscope by JEOL, with the accelerating voltage of 300 kV and maximum magnification of 300 000x. Thin foils were made in the longitudinal section, by cutting out approx. 0.5 mm thick inserts from solid specimens, and then discs with the diameter of 3 mm were cut out from them using an ultrasound drill. The discs were initially ground mechanically to the thickness of approx. 90 μm and an approx. 80 μm deep groove was polished. Finally, the preparations were subjected to ion thinning with a device by Gatan company.

The phase composition analysis of substrates and coatings was performed with the X-ray diffraction method with an X´Pert Pro X-ray device by Panalytical with the Bragg-Brentano configuration using the filtered radiation of a cobalt lamp with the rated voltage of 40 kV and the filament current of 30 mA. A 0.05^{o} step and with the pulse counting time of 10 seconds was assumed. As the reflexes of the substrate material and coating are overlapping and considering their intensity making it difficult to analyse the results obtained, the razing-incidence X-ray

diffraction method for the primary X-ray beam using a parallel beam collimator before a proportional detector was used in further investigations to obtain more accurate information from the analysed material surface layer. As a diffraction pattern can be recorded with the low incidence angles for the beam onto the specimen surface, diffraction patterns from thin layers can be obtained by increasing the volume of the material taking part in diffusion. The diffraction patterns of graded and multilayer coatings were established for the different incidence angles of the primary beam.

Variations to the chemical concentration of coating components in the direction perpendicular to its surface and concentration changes in the transient zone between the coating and the substrate material were evaluated with tests performed with a GDOES-750 QDP glow discharge optical spectrometer by Leco Instruments. The following working conditions of the spectrometer's Grimm lamp were determined in the tests: inner lamp diameter 4 mm, lamp supply voltage 700 V, lamp current 20 mA, working pressure 100 Pa.

The thickness of the coatings deposited was measured with a "kalotest" method consisting of measuring the characteristic sizes of a crater formed through wear on the surface of the tested specimen with a steel ball with the diameter of 20 mm. A suspension of diamond grains with the diameter of 1 μm was supplied between the rotating ball and the specimen surface. The test time of 120 seconds was set. The wear size was measured through observations with an MEF4A Leica metallographic light microscope. The coating thickness was determined according to the following relationship:

$$g = \frac{D \cdot (D - d)}{4 \cdot R} \cdot 10^3 \tag{1}$$

where:

g – coating thickness, μm,

D – outer crater diameter, mm,

d – inner crater diameter, mm,

R – ball radius, mm.

5 measurements for each of the tested specimens were made to obtain the average thickness values for the measured coatings. In addition, to verify the results obtained, the thickness of the coatings was measured with a scanning electron microscope on the transverse fractures of specimens.

Surface roughness for the polished samples without coatings and with coatings was measured in two mutually perpendicular directions with a Surftec 3+ profilometer by RankTaylor Hobson. The measurement length of l = 0.8 mm and the measurement accuracy of ±0.02 μm was assumed. In addition, to confirm the results obtained, surface roughness measurements for the specimens were made with an LSM 5 Exciter confocal microscope by Zeiss. The R_a parameter acc. to PN-EN ISO 4287:2010 was adopted as a value describing surface roughness.

The hardness of the materials tested was determined using the Vickers method. The hardness of the coated substrates made of sintered tool materials was tested using the Vickers method according to PN-EN ISO 6507-1:2007. The microhardness tests of the deposited coatings were conducted with a Future Tech microhardness tester with the dynamic Vickers method. The load of 0.98 N (HV0.1) was used that allows to eliminate, as far as possible, the impact of the substrate on the results obtained. The measurements were made in the periodical loading and unloading mode, where the tester is loading the indenter with the set force, maintains the load for certain time, and then unloads it. Dynamic hardness is determined according to the following formula [20]:

$$DH = \alpha \cdot \frac{P}{D^2} \tag{2}$$

where:

α – a constant expressing the indenter shape impact, for Vickers α = 3.8584,

P – set load, mN,

D – indention depth, μm.

The test allows to observe variations to the plastic deformation and elastic deformation of the tested material, respectively during loading and unloading owing to the precision measuring system recording the depth of the indention formed in the individual phases of the test. The measurements were made by making 6 indentions for each of the tested specimens.

The adherence of the deposited coatings to the tested sintered tools materials was assessed with a scratch – test with REVETEST equipment by CSEM. The method consists of moving a diamond Rockwell C indenter along the specimen surface with a constant speed with the loading force rising proportionally to displacement. The tests were made within the pressing force range of 0-200 N, growing with the speed of (dL/dt) = 100 N/min at the distance of 10 mm.

The L_c critical load at which coating adherence is lost was determined according to the acoustic emission (AE) value registered during a measurement and by observing the scratches formed during a scratch test. The character of the damage was assessed based on observations with a Zeiss Supra 35 scanning electron microscope and with an LSM 5 Exciter confocal microscope by Zeiss.

Abrasive wear resistance tests and the wear factor tests for the tested coatings were performed with the pin-on-disc method with a CSEM High Temperature Tribometer (THT) linked directly to a PC allowing to define the size of load, rotation speed, radius in the specimen, maximum friction coefficient, test duration. A 6 mm wolfram carbide ball was used as a counter-specimen. The tests were made at a room temperature under the following test conditions: pressure force of $FN = 5$ N, movement speed of $v = 0.1$ m/s, radius of $r = 5$ mm.

The functional properties of the deposited coatings were determined with technological cutting tests at a room temperature. The cuttability tests of the tested tool materials without coatings and with the deposited coatings were carried out with a continuous rolling test without the use of the working cooling and lubricating liquids. The tool life of the tested inserts was determined by measuring the wear track width on the tool flank through measuring the VB average wear track width after cutting in a specific time interval. Cutting tests were interrupted when the VB value exceeded the set criterion. For uncoated tools, the test was made to achieve the wear criterion, and the test duration for tools with the deposited coatings was not shorter than for the uncoated tools, thus enabling to compare of VB wear track width after fulfilling the wear criterion by the uncoated specimen. VB measurements were made using a light microscope.

Technological cutting tests for the tested sintered tool materials was carried out under varied conditions and on the varied treated material, corresponding, as much as possible, to the operating requirements concerning the individual groups of substrate materials and also the coatings applied. A model of artificial neural networks was developed to evaluate the effect of coatings properties such as substrate adherence, microhardness, thickness and grain size on the operating life of the coated cutting edges.

2.2. Foresight methodology

In order to determine the strategic position of PVD and CVD technology against materials surface engineering, reference data was used acquired as a result of performing foresight research under the "Foresight of surface properties formation leading technologies of

engineering materials and biomaterials FORSURF" project [79]. Nearly 300 independent foreign and domestic experts representing scientific, business and public administration circles who have completed approx. 600 multi-question surveys and held thematic discussions during 7 workshops took part in the FORSURF technology foresight up till now at the different stages of works. Development prospects for about 500 groups of specific technologies were analysed in the initial phase of the research including the evaluation of the state of the art, technology review and strategic analysis with integrated methods. The following scientific and research methods were applied for this purpose: extrapolation of trends, environment scanning, STEEP analysis, SWOT analysis, expert panels, brainstorming, benchmarking, multi-criteria analysis, computer simulations and modelling, econometric and static analysis. 14 thematic areas with 10 critical technologies were chosen as a result of the works, being the priority technologies of materials surface engineering with the best development prospects and/or of crucial importance in the industry in the next 20 years. A collection of 140 critical technologies were thoroughly analysed according to three iterations of the Delphi method carried out in consistency with the idea of e-foresight [12] using information technology encompassing a virtual organisation, web platform and neural networks. Neural networks were used in a novel and experimental manner to analyse the crossing influence showing relationships between the analysed trends and events likely to occur in the future within the considered timeframe.

The specific detailed technologies analysed in this chapter were evaluated based on experts opinions using the custom foresight research methodology [11]. A universal scale of relative states being a single-pole scale without zero was used in the research undertaken, where 1 is a minimum rate and 10 an extraordinarily high rate. Homogenous groups should be differentiated between for the technologies analysed in the first place according to the adopted handling procedure in order to subject such technologies to planned experimental and comparative investigations. The individual groups of the technologies were evaluated for their potential representing a realistic objective value of the specific group of technologies and for attractiveness reflecting the subjective perception of a specific technology by its potential users. The results were entered into one of the quarters of the **dendrological matrix of technology value** serving to visualise the objectivised values of the specific separated groups of technologies. A wide-stretching oak is the most promising quarter guaranteeing the future success. A soaring cypress and a rooted dwarf mountain pine may also ensure success provided an appropriate procedure is applied, which is unlikely or impossible for a quaking aspen. **The**

metrological matrix of environment influence presents graphically the results of evaluation for the influence of external positive factors (opportunities) and negative factors (difficulties) on the technologies analysed. Each of the technologies groups assessed by the experts was entered into one of the matrix quarters. Sunny spring illustrates the most favourable external situation ensuring the future success. Rainy autumn, providing a chance for steady progress, corresponds to a neutral environment and hot summer to a stormy environment where the success of a technology is risky but feasible. Frosty winter informs that technology development is difficult or impossible. The results of the expert investigations visualised with the dendrological and meteorological matrix were at the next stage of scientific work entered into the **matrix of strategies for technologies** by means of software based on the previously formulated mathematic relationships [11]. The matrix presents graphically a place of each group of technologies according to its value and environment influence intensity and identifies a recommended action strategy. The **strategic development tracks** were applied onto the technology strategy matrix consisting of sixteen fields reflecting the predicted situation of the given technology if positive, neutral or negative external circumstances occur. The forecast established concerns the time intervals of 2015, 2020, 2025 and 2030 and presents a vision of future events consisting of several variants.

3. Materials science research results

3.1. Substrates structure

Observations with an electron scanning and transmission microscope have revealed that the tested sintered tool materials are characterised by a well densed, compact structure with no pores (Figs. 1, 2). Besides, fracture surface topography for oxide and nitrogen ceramics signifies high brittleness, characteristic for oxided ceramic materials (Fig. 3). The occurrence of the relevant elements in the substrate structure of the tested sintered tool materials was confirmed with the EDS chemical composition analysis (Fig. 4).

The phase composition of the tested substrate materials according to the assumptions confirmed with the tests held with the X-ray qualitative phase analysis method. Fig. 5 presents an X-ray diffraction pattern for the Al_2O_3+TiC ceramics substrate and Fig. 6 shows an X-ray diffraction pattern for sialon ceramics.

Figure 1. *A-type sintered carbide thin foil structure*

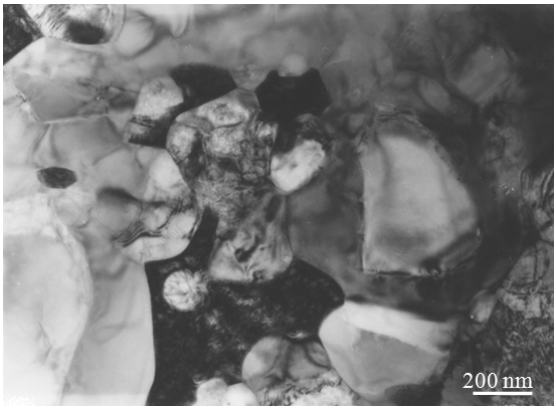

Figure 2. *A-type cermet thin foil structure*

3.2. Structure, chemical and phase composition of coatings

It was found based on the fractographic tests made with a scanning electron microscope that the coatings deposited evenly onto the tested substrate made of cemented carbides, cermet or tool ceramics are characterised by the thickness of 0.8-12.5 μm (Fig. 7, Table 2). All the PVD and CVD coatings deposited onto the substrates made of sintered tool materials are characterised by a structure free of pores, cracks and discontinuities**.** The layer structure of coatings was observed for multilayer coatings and step-graded coatings. The individual layers are characterised by a homogenous thickness within the entire observation area and tight adherence to each other and of the whole multilayer coating to the substrate (Figs. 7-10).

For the coatings deposited with the CVD method onto the substrate made of tool Si_3N_4 nitride ceramics and sialon ceramics with a TiN layer in the surface zone, the observations of the surface morphology have shown that heterogeneities exist related to the occurrence of multiple pores on the substrate and the networks of microcracks characteristic for such process. In case of Ti(C,N)+TiN and TiC+TiN coatings, single minor ball-shaped microparticles can be observed on their surface. When an Al_2O_3 layer is on the substrate surface, however, or if this layer is in the under-the-surface zone (upper TiN layer is very thin), then the particles are shaped polyhedrally (Fig. 11).

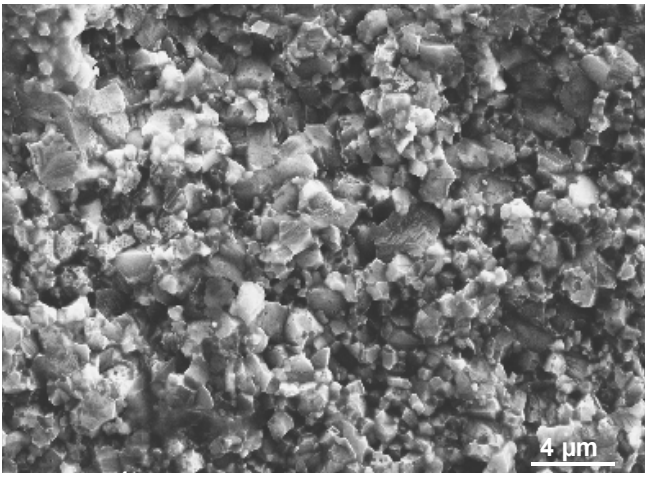

Figure 3. *Fracture surface of the Al_2O_3+TiC oxide ceramics substrate*

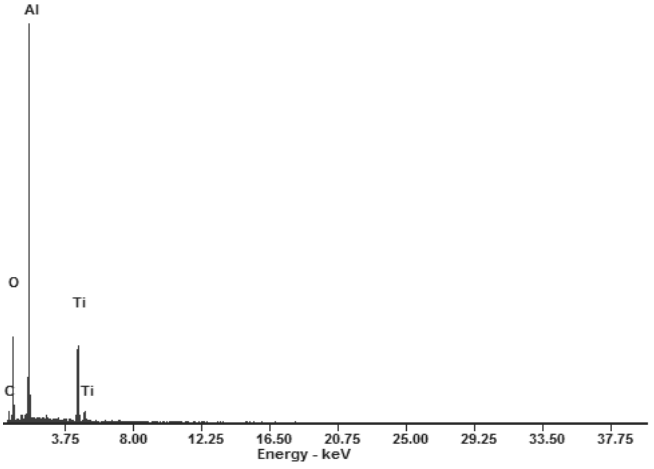

Figure 4*. The X-ray energy dispersive plot of the area, according to Fig. 3*

The observations of morphology of coatings deposited in the PVD process on the cemented carbides, cermets and oxide ceramics substrate reveal a high heterogeneity related to the occurrence of multiple droplet-shaped microparticles (Figs. 12, 13). The morphological defects observed created when depositing a coating are most probably a result of splashing the titanium droplets removed from a titanium disc against the substrate surface as confirmed by an EDS test from microregions (Fig. 14).

The correct phase composition of the tested coatings was found as a result of thin foils tests with an electron transmission microscope, however, as the TiN and Ti(C,N) phases are isomorphic, the diffraction differentiation of each of the phases is impossible. The structure of step-graded coatings is fine-grained (as signified by, in particular, the clear rings of reflexes on diffraction images). The individual layers cannot be identified with the electrons diffraction method also for coatings containing Ti(C,N), Ti(B,N) and TiN layers due to isomorphism of such phases and the approximate network parameter value. Fig. 15 presents the structure of thin foils made of the Ti(B,N) coating on the sialon substrate and diffraction patterns. A continuous analysis between the coating and the substrate was performed in the spectrometer of the scattered X-ray radiation energy to confirm the occurrence of chemical composition gradient in the (Ti,Al)N, Ti(C,N) coatings (Figs. 16, 17). The character of changes to the concentration of the elements forming the coatings shows their gradient structure.

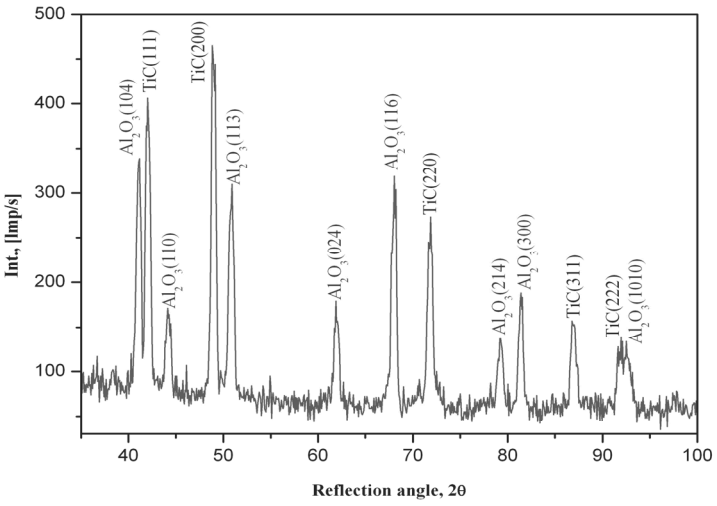

***Figure 5**. The X-ray energy dispersive plot of the Al_2O_3+TiC ceramics substrate (Bragg-Brentano geometry)*

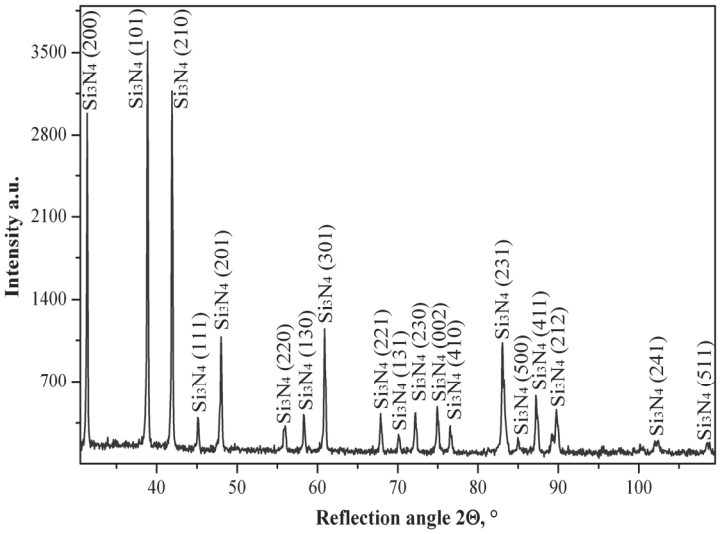

***Figure 6**. The X-ray energy dispersive plot of the sialon ceramics substrate*

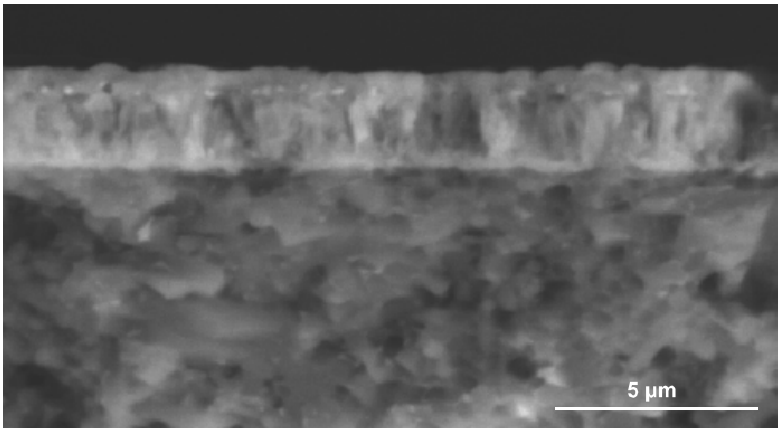

***Figure 7**. Fracture of the Ti(C,N)+TiN multilayer CVD coating deposited onto the Si_3N_4 substrate*

Figs. 18 and 19 illustrate variations to the mass concentration of coatings components and substrate material depending on the numbers of coatings deposited made with the Glow Discharge Optical Emission Spectroscopy GDOES. The investigations only allow to identify quality variations to chemical composition in the chosen microarea of each specimen. The recurrent distribution of elements forming part of the coatings and the substrate was determined.

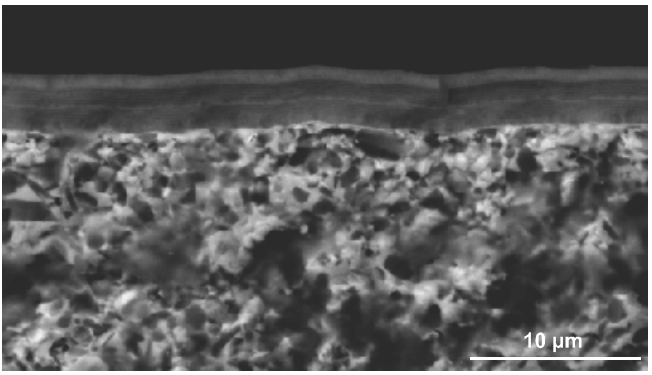

***Figure 8**. Fracture surface of the TiN+multiTiAlSiN+TiN multilayer coating deposited onto the cermet substrate*

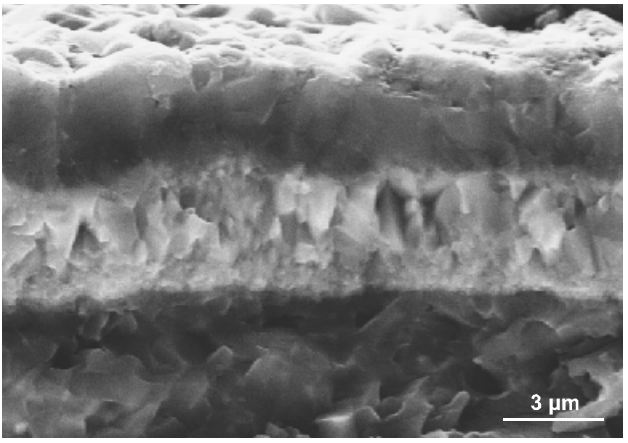

***Figure 9**. Fracture surface of the Ti(C,N)+Al_2O_3+TiN multilayer CVD coating deposited onto sialon ceramics*

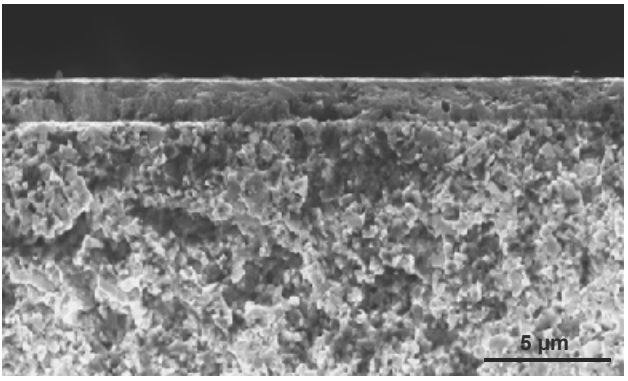

***Figure 10**. Fracture surface of the Ti(C,N) monolayer, complex, nanocrystalline coating deposited onto B-type cemented carbides*

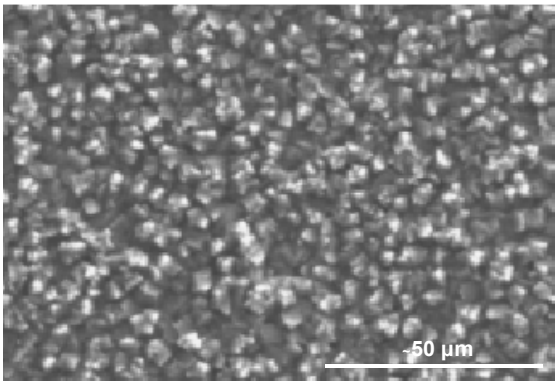

Figure 11. *Surface topography of the TiN+Al_2O_3 multilayer CVD coating deposited onto the Al_2O_3+$SiC_{(w)}$ substrate*

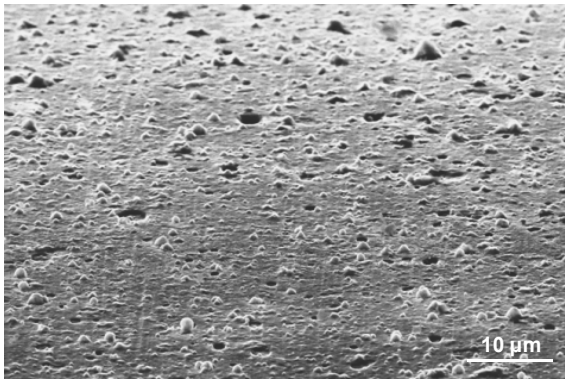

Figure 12. *Topography of the Ti(C,N) graded coating deposited onto the cermet substrate*

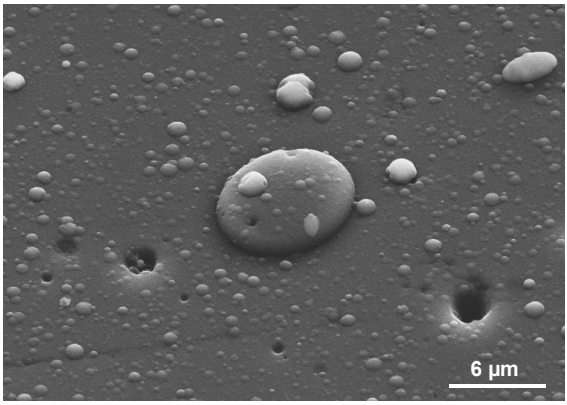

Figure 13. *Topography of the Ti(C,N) (1) continuous graded coating deposited onto sialon ceramics*

a)

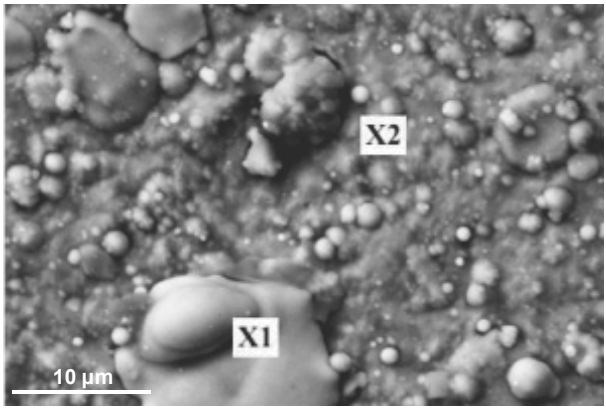

b)

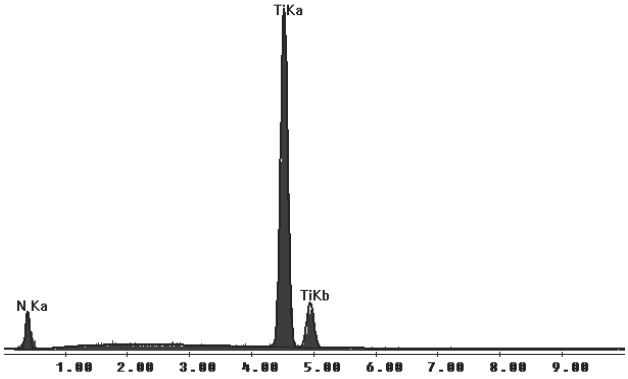

c)

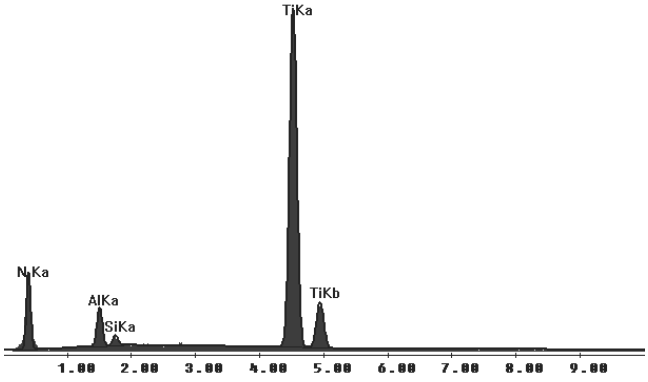

Figure 14. *a) Surface topography and the X-ray energy dispersive plot of the TiN+multi(Ti,Al,Si)N+TiN multilayer coating surface microareas deposited onto the Si_3N_4 nitride ceramics – b) X1 area, c) X2 area*

a)

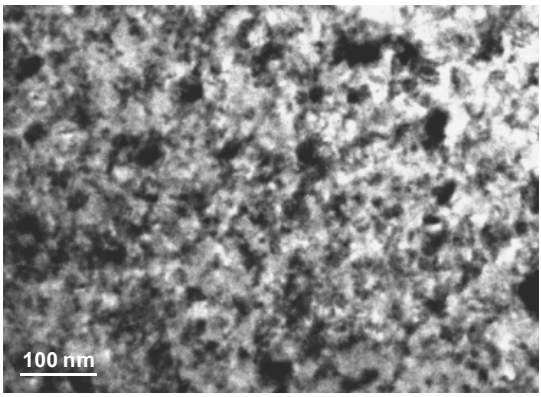

b)

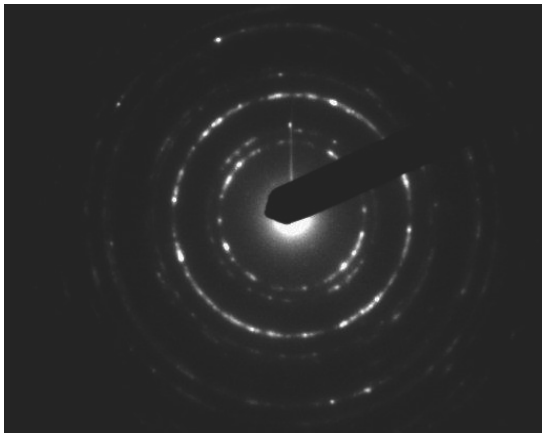

c)

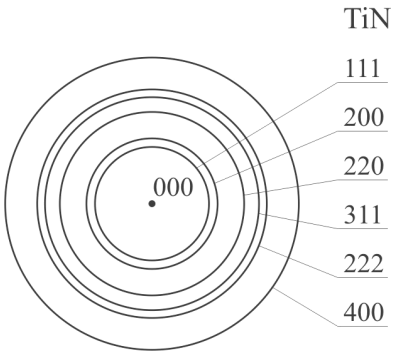

***Figure 15**. The structure of the Ti(B,N)continuous graded coating deposited onto tool sialon ceramics, a) image in light field, b) diffraction pattern from the area as in Fig. a, c) diffraction pattern solution from Fig. b*

It was determined with the X-ray qualitative phase analysis methods that, as assumed, coatings were deposited on the surface of the investigated tool materials containing TiN, TiC and Ti(C,N) type phases for the PVD coatings and TiC, Ti(C,N), Al_2O_3 and TiN phases for the CVD coatings. They could not be distinguished between according to diffraction due to the isomorphism of TiN phases with Ti(B,N), (Ti,Zr)N and (Ti,Al)N phases. The reflexes of phases coming from the substrates were also identified on X-ray diffraction patterns, especially for inserts with the PVD coatings. This results from a small thickness of the coatings applied on the investigated sintered tool materials smaller than the material penetration depth of X-ray radiation beams (Fig. 20).

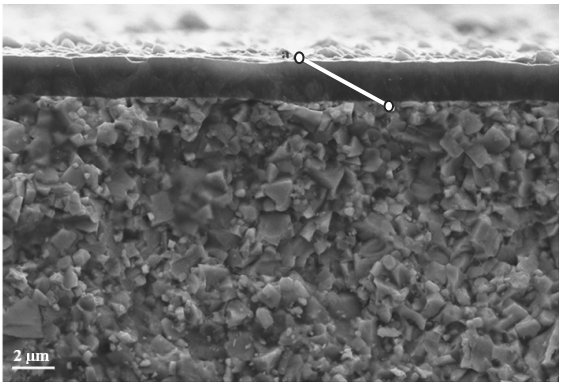

Figure 16. *Fracture surface of the Ti(C,N) continuous graded coating deposited onto the cemented carbides*

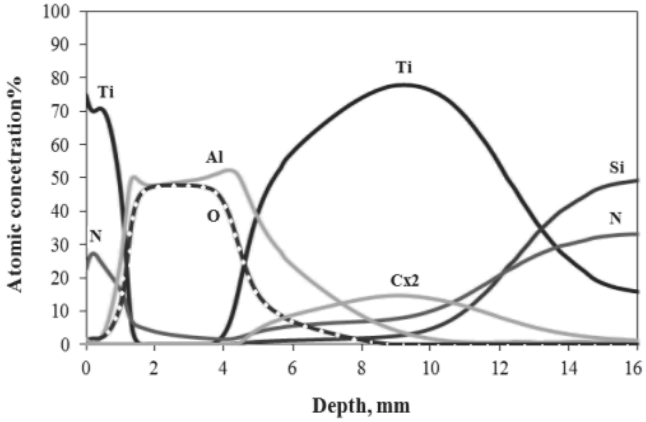

Figure 18. *Variations to the concentration of components of the Ti(C,N)+Al_2O_3+TiN multilayer CVD coating and the Si_3N_4 nitride ceramics substrate analysed with a GDOES spectrometer*

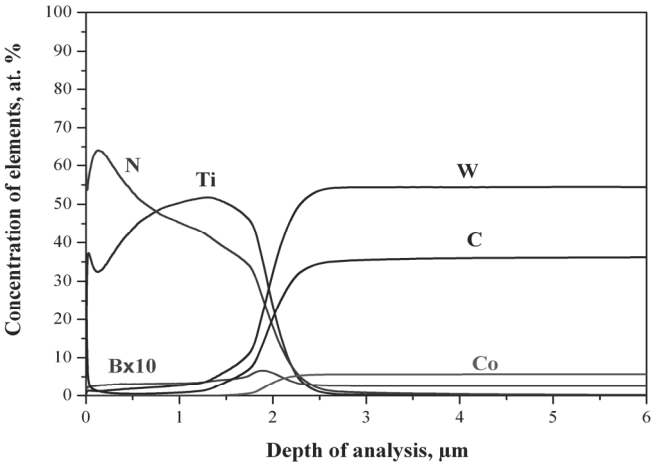

Figure 19. *Variations to the concentration of components of the Ti(B,N) multilayer coating and the substrate material made of A-type cemented carbides with a GDOES spectrometer*

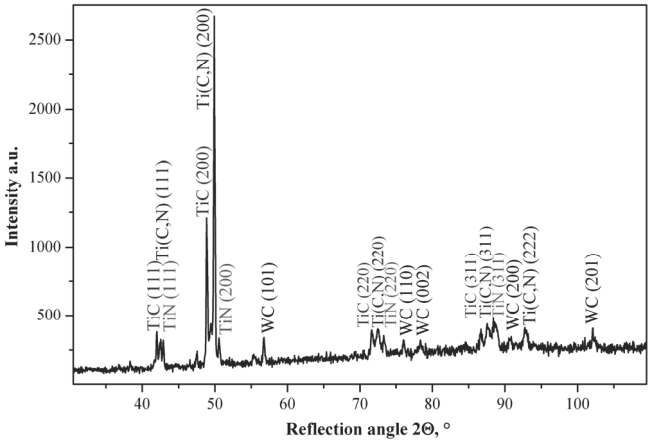

Figure 20. *The X-ray energy dispersive plot of the Ti(C,N)+TiN multilayer CVD coating deposited onto A-type cemented carbides (Bragg-Brentano geometry)*

Reflexes from the thin surface layers were only registered as a result of investigations with the GIXRD – grazing incident X-ray diffraction technique for the low incident angles of the primary X-ray beam (Fig. 21). The lack of reflexes from the phases occurring in the substrates on the diffraction patterns prepared with the GIXRD technique signify that an X-ray beam penetrating the tested coatings did not permeate to the substrate.

a)

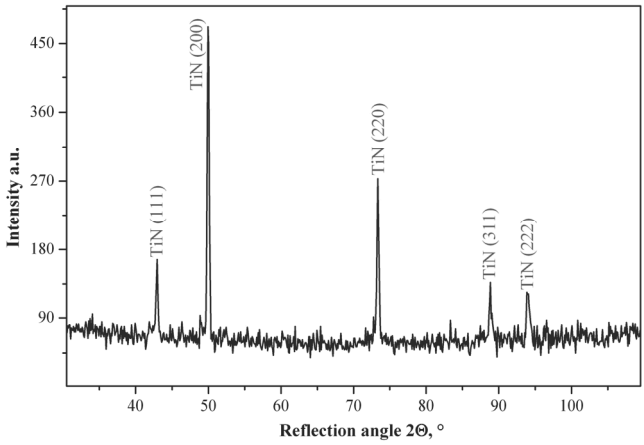

b)

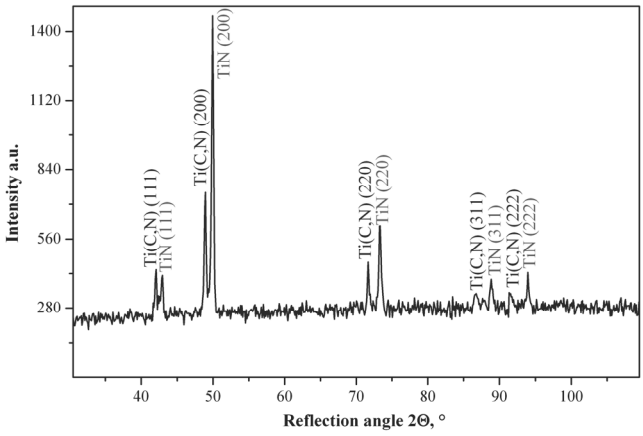

***Figure 21**. The X-ray energy dispersive plot of the Ti(C,N)+TiN multilayer CVD coating deposited onto A-type cemented carbides prepared with the grazing incident X-ray diffraction technique (GIXRD): a) α = 0.1°; b) α = 4°*

3.3. Mechanical and functional properties

It was found by measuring the thickness of coatings with the "kalotest" method that that the largest thickness exhibit those of the investigated coatings deposited with the CVD method (up to 12.5 μm for the Ti(C,N)+Al_2O_3+TiC coating deposited onto the B-type cemented carbides substrate). The thickness of coatings deposited with the PVD method is below 1 μm for the

majority of simple monolayer coatings and between 1.1 μm to 5.0 μm for multilayer and graded coatings. The majority of the investigated coatings is characterised by the thickness of 2-3 μm, which is an optimum value allowing to use the antiwear properties of the coating while maintaining its good adherence.

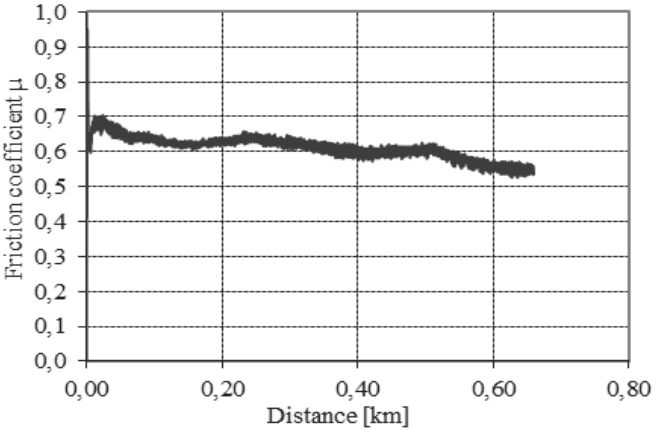

***Figure 22**. Interdependence between the friction factor and the friction distance in pin-on-disc test of the TiN+(Ti,Al,Si)N+ (Al,Si,Ti)N step-graded coating deposited onto the Al_2O_3+$SiC_{(w)}$ substrate*

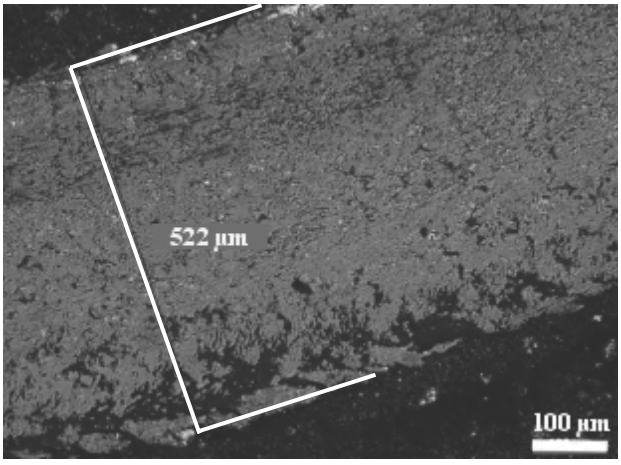

***Figure 23**. Measurement of the tribological damage track width on the surface of the TiN+(Ti,Al,Si)N+(Al,Si,Ti)N step-graded coating deposited onto the Al_2O_3+$SiC_{(w)}$ substrate*

The roughness tests carried out have shown that the monolayer, complex nanocrystalline coatings (0.12 μm to 0.27 μm) reveal the relatively lowest roughness parameter in terms of materials with the monolayer coatings. For the multilayer coatings, the lowest roughness parameters occur for the CVD coatings except for the coatings containing Al_2O_3, where the parameter is rising due to the polyhedral nature of the coating topography. The lowest roughness parameter values for the graded coatings have been recorded for the Ti(C,N) continuous graded coatings deposited on the "B" type cemented carbides and cermet substrate. It was pointed out that the heterogeneities of the coating surface related to the presence of titanium droplets removed from the disc during the cathode arc evaporation have a significant effect on the roughness of the investigated coatings. Despite such heterogeneities, the roughness parameter values remain at the level enabling effective tool work and do not largely increase the friction factor as confirmed in pin-on-disc tests (Figs. 22, 23).

The investigated coatings are characterised by high microhardness, which is important in terms of applications due to the functions fulfilled connected with, in particular, limited mechanical wear. The largest microhardness for the monolayer coatings is exhibited by the complex monolayer coatings (the 3580 HV and 3340 HV for the (Ti,Al)N coating deposited onto the Al_2O_3+TiC and Al_2O_3+$SiC_{(w)}$ oxide ceramics substrate). The largest percentage growth in microhardness to the substrate material was noted for such materials (respectively, 85% for the (Ti,Al)N monolayer complex coating deposited onto the Al_2O_3+TiC ceramic substrate and 82% for the monolayer (Ti,Al)N complex substrate deposited onto the Al_2O_3+ $SiC_{(w)}$ ceramic substrate). In case of the multilayer coatings, the largest microhardness is exhibited by the TiN+multi(Ti,Al,Si)N+TiN multilayer coatings with more than 10 layers deposited onto the Al_2O_3+ZrO_2, Al_2O_3+TiC and Al_2O_3+ $SiC_{(w)}$ oxide ceramics substrates (respectively, 4050 HV, 3980 HV and 3970 HV). The largest growth of microhardness versus the uncoated materials was noted also for such materials (respectively, 121%, 105% and 116%). The highest microhardness for the graded coatings have the (Ti,Al)N continuous graded coatings on A-type cemented carbides, (Ti,Al)N on the Al_2O_3+TiC oxide ceramics substrate, and (Al,Ti)N on the sialon ceramic substrate (respectively 3327 HV, 3200 HV and 3600 HV). The highest microhardness increase for the graded coatings against the uncoated material was seen for coatings featuring the highest hardness (82% for the (Ti,Al)N coating on the A-type cemented carbides substrate and 77% for the (Al,Ti)N coating on the sialon ceramics substrate) but also for the (Al,Ti)N coating deposited onto the A-type cemented carbides substrate (81% increase).

It was found out that no matter if the tested coatings had been applied as monolayer, multilayer or graded coatings, the hardness of the Ti(C,N) coatings with the presence of metallic TiN and TiC phases show smaller hardness than the (Ti,Al)N or (Ti,Al,Si)N coatings where, both, metallic TiN bonds and covalence AlN bonds exist. If wear resistant coatings are deposited onto the tested substrates, a clear increase in surface layer microhardness is seen, thus contributing to the lower wear intensity of the cutting tools edge made of cemented carbides, cermets, oxide ceramics, nitride ceramics and sialon ceramics during cutting. Fig. 24 presents the highest results for microhardness measurements obtained for the individual groups of coatings.

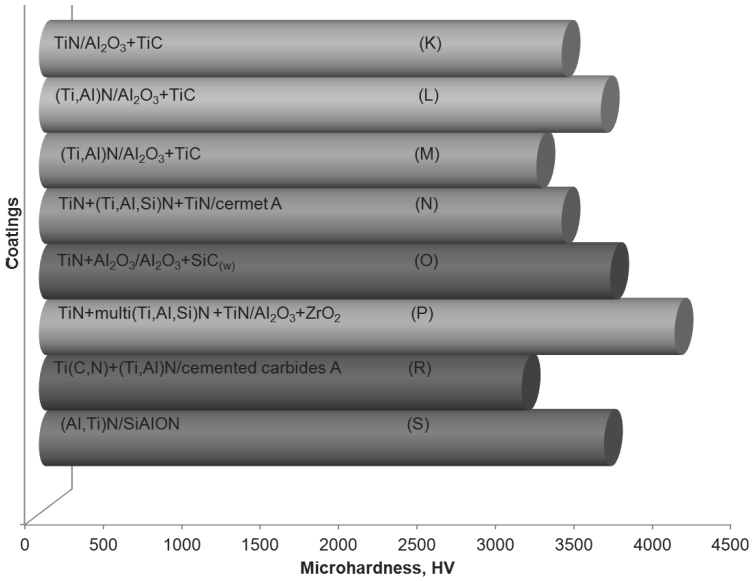

***Figure 24**. The highest results for microhardness measurements obtained for the individual groups of coatings*

The coatings subject to the research are distinctive for their good adherence to the substrate except for the single CVD coatings deposited onto the oxide ceramics substrates, which may be connected with the substrate material being very stable chemically. The best adherence for the monolayer coatings was determined for the classical complex coatings (54-99 N), in addition, very good adherence (over 40 N) was found out also for all the complex monolayer, nanocrystalline coatings. Different L_c critical load values (15 to 131 N) were recorded for the multilayer coatings, multilayer coatings with the number of layers more than 10 are

characterised by very good adherence only (over 40 N) (Fig. 25). Different L_c critical load values were recorded for the graded coatings, whereas the highest adherence is exhibited by the (Al,Ti)N and (Ti,Al)N continuous graded coatings on A-type (Al,Ti)N cemented carbides on sialon ceramics. The highest results for critical load obtained for the individual groups of the coatings investigated are shown in Fig. 26.

The coating damages formed as a result of adherence tests with the scratch method were made on the basis of observations in a scanning microscope and confocal microscope (Fig. 27). It was found out as a result of the observations that the damages to the PVD coatings are of the abrasive wear nature, and are also characterised by a high number of single or double coating cracks at the scratch peripheries and delamination inside the scratch leading to coating delamination where it contacts the scratch. An increasing load during the scratch test leads to intensified cracks at the edge peripheries, leading to partial coating delamination. The periodical chipping of coatings can be also observed.

It was stated in an analysis using a model of artificial neural networks that the tool life of the sialon ceramic and cemented carbides tools deposited with the examined coatings depends mainly on the adherence of the coatings to the substrate, and hardness, grain size and grain thickness have a smaller effect on the tool life (Fig. 28).

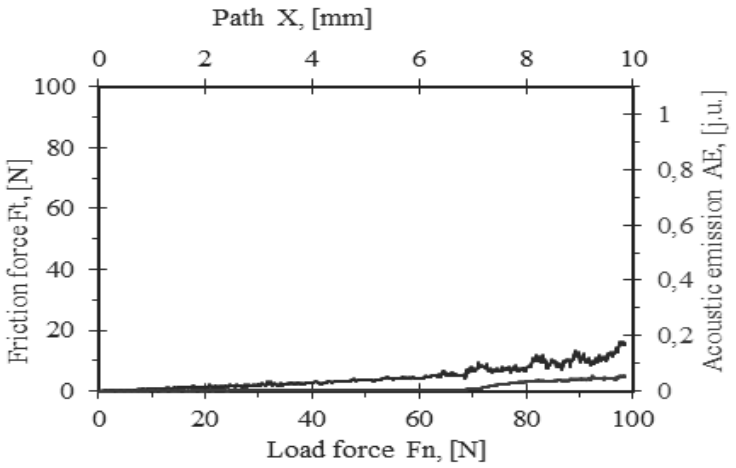

***Figure 25**. Record of scratch test curve for the TiN+multi(Ti,Al,Si)N +TiN multilayer coating deposited onto the Al_2O_3+TiC substrate*

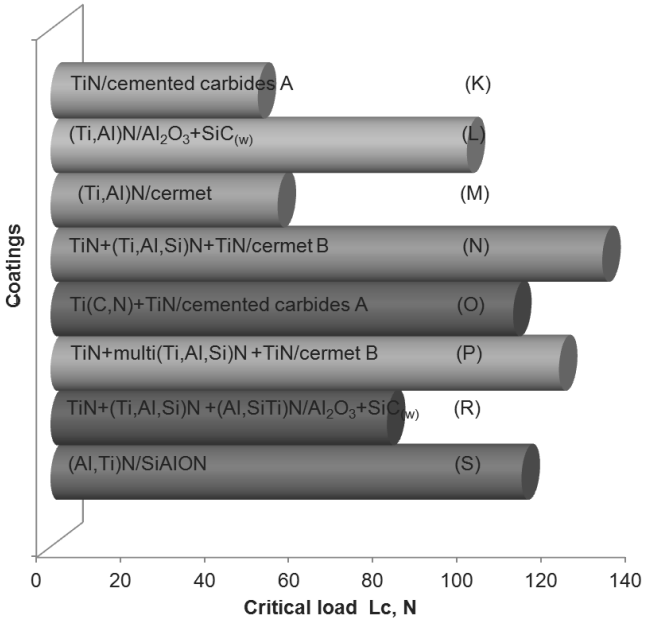

***Figure 26**. The highest results for critical load obtained for the individual groups of coatings*

It was stated as a result of the carried out technological cutting tests that the TiN monolayer, simple coating deposited onto the A-type cemented carbides substrate shows the largest relative growth of tool life for the monolayer coatings as compared to uncoated material. It was found out by comparing the average growth of tool life for the specific types of the monolayer coatings that the growth is largest for the monolayer, complex, nanocrystalline coatings (300%). The very high, relative growth of tool life was also achieved for the monolayer, complex, classical coatings (140%). It should be noticed here that the high result of relative tool life growth obtained for the complex monolayer coatings is especially more important that it had been achieved for materials with a ceramic substrate which, regardless the coating applied, feature very high resistance to wear. The highest relative growth of tool life for the multilayer coatings was achieved for the multilayer PVD coatings deposited onto the A-type sintered carbide substrate with the number of layers more than 10: 2700% for the TiN+multi(Ti,Al,Si)N+TiN coating and 2150% for the multi (Al,Cr)N coating. The highest relative growth of tool life was also obtained for the multilayer PVD coatings with more than 10 layers (685%). The highest relative growth of tool life in the group of the graded coatings was achieved for the continuous (Ti,Al)N, (Al,Ti)N and Ti(C,N) graded coatings deposited

a)

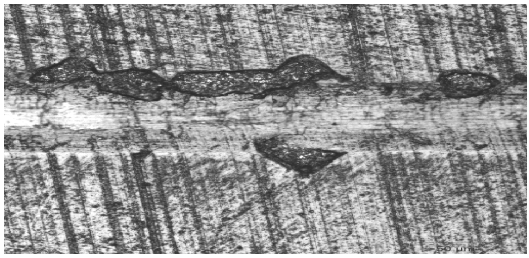

b)

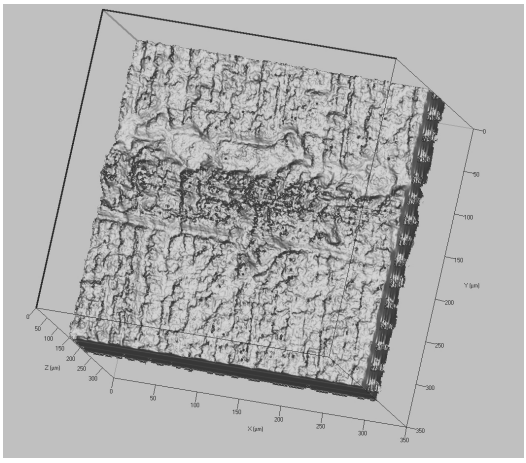

c)

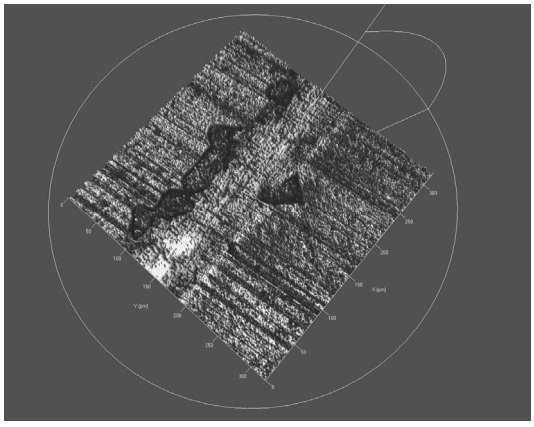

Figure 27*. a) Damage characteristic of the (Ti,Al)N monolayer, complex, nanocrystalline coating deposited onto the B-type cemented carbides substrate in a scratch test curve, b) 3D model, c) surface topography of the damaged coating, viewed with a confocal microscopy*

onto the A-type cemented carbides substrate (respectively, 2900%, 2650% and 2550%). The relative average growth of tool life for the graded coatings was also achieved for the continuous graded coatings (715%). A qualitative relationship was identified between the microhardness results collected and adherence to the substrate and the tested materials' operating properties, in particular the relative growth of wear resistance for the coated material as compared to uncoated material.

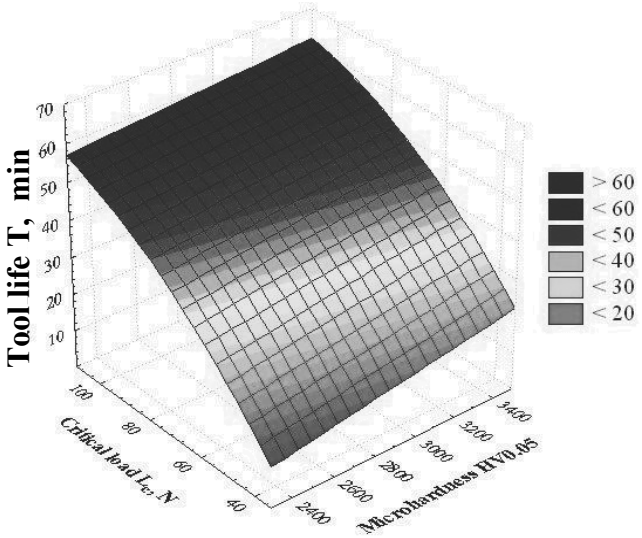

Figure 28. *Evaluation of the effect of critical load and microhardness of the PVD and CVD coatings on tool life for the cemented carbides tools coated with the PVD and CVD coatings determined with the SSN method for the set coating depth of 2.5 μm and grain size of 9.8 nm*

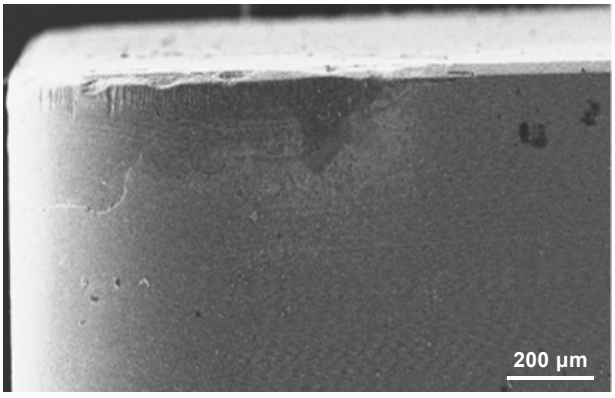

Figure 29. *Characteristic wear of the tool flank of the Al_2O_3+TiC oxide ceramic insert with the (Ti,Al)N monolayer, complex, nanocrystalline coating deposited*

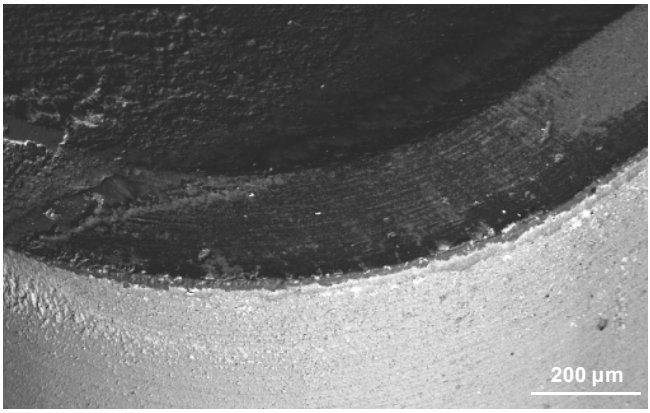

***Figure 30**. Characteristic wear of the tool flank of the Si_3N_4 ceramic insert with the Al_2O_3+TiN (2) multilayer CVD coating deposited*

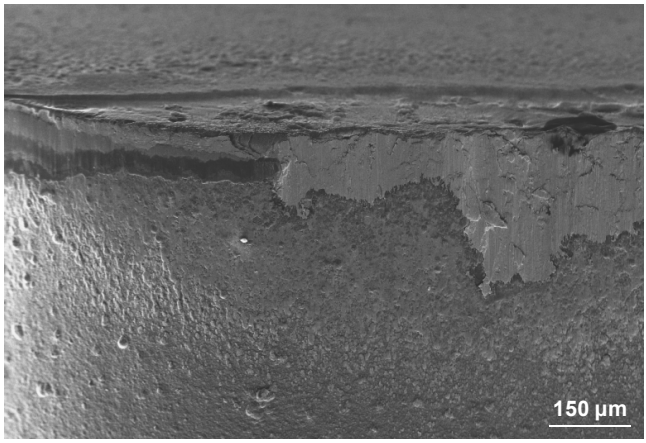

***Figure 31**. Characteristic wear of the tool flank of the A-type cemented carbides plate with the Ti(C,N)+Al_2O_3+TiN multilayer CVD coating deposited*

It was found out as a result of examining the topography of a worn tool surface with a scanning electron microscope that the most common types of tribological damages identified for the examined materials are mechanical and abrasive damages to the tool flank, a crater formed at the tool flank, cracks on the tool flank and cutting edge chippings (Figs. 29-31).

Due to the cutting parameters different according to the substrate material used in the technological cutting test, it is not possible to compare the machining quality obtained for the specific groups of coatings, a qualitative relationship can be however pointed out between the mechanical properties results obtained (including microhardness and adherence), tool life and

treatment quality measured as the roughness of the workpiece. The high wear resistant of the edge, combined with high coating microhardness and its good adherence to the substrate is accompanied by a relatively low roughness of the cutted material. This should be linked to the better removal of chippings ensured with the coating applied and with the limited formation of buildup on the coated surface of the edge. The detailed results of studies into the structure and properties of sintered tool materials with the PVD and CVD coatings deposited are shown in Table 2.

4. PVD/CVD development perspectives

4.1. PVD/CVD technologies versus surface engineering development

Foresight investigations with the sample size of 198 have revealed that PVD technologies have a strong strategic position among other materials surface engineering technologies. The future role of CVD technology was appraised by independent domestic and foreign experts representing scientific, business and public administration environments. According to 61% of respondents, PVD technologies are in the group of technologies with the best prospects of industrial applications, and CVD technologies according to 46% of respondents. A large group of experts maintain that scientific and research works will be frequently devoted in the nearest 20 years to the concept of physical and chemical vapour deposition. 47% and 35% of the surveyed, respectively, held such a view. Nearly a half of the surveyed (48%) claim that the thematic area of "PVD technologies" is crucial and its importance should be absolutely rising so that an optimistic scenario can come true of the country's development – "Race won" – assuming that the potential available is adequately utilised to fulfil the strategic objectives of development and so that people, statistically, are better off, social attitudes are optimistic and prospects for the coming years bright. 37% of the surveyed persons share such a view with regard to CVD technologies. 51% of the surveyed assert that the significance of PVD technologies in relation to other materials surface engineering technologies will be growing, whereas 47% maintain it will remain on the same level, with only 2% claiming that the importance will diminish over the next 20 years. The anticipated role of CVD technologies was valued somewhat lower by experts. 54% of them point out that the role of CVD technologies in the nearest 20 years in respect of other surface engineering technologies will remain at the current

level, while 39% argue it will be growing and 7% think it will be shrinking. The presented results of foresight research elaborated with reference data point to the anticipated role of PVD technologies and a somewhat smaller role of CVD technologies in the development of materials surface engineering in general (mezo scale) and development of Poland's overall economy (macro scale).

4.2. Strategic position of the specified PVD/CVD technologies

The results of the foresight research described in this chapter include the assessment of the potential and attractiveness of the analysed technologies against the micro- and macro-environment performed based on the key experts' opinions expressed in a ten-degree universal scale of relative states and a recommended strategy of managing a relevant technology resulting from the assessment together with the predicted strategic development tracks. The individual technology groups have been evaluated by experts using a ten-degree universal scale of relative states for their: business, economic, humane, natural and system attractiveness as well as for their creational, applicational, qualitative, developmental and technical potential. A weighted average for the criteria considered (attractiveness and potential) was calculated using a multi-criteria analysis, and a result obtained for the individual groups of technologies was entered into the dendrological matrix of technologies value (Fig. 32). An analysis made revealed that the most attractive technology having the greatest potential is the physical vapour deposition of the multilayer coatings with the number of layers of $n \geq 10$ (P), continuous graded coatings (S) and complex, nanocrystalline monolayer coatings (M) that were qualified to the matrix quarter called a wide-stretching oak. The technologies with a high potential and limited attractiveness include the physical vapour deposition of the complex, classical monolayer coatings (L) and multilayer coatings with the number of layers of $n<10$ (N) qualified to the quarter of the matrix called a rooted dwarf mountain pine. The quarter called soaring cypress with highly attractive technologies having a limited potential includes the physical vapour deposition of the step-graded coatings (R). The physical vapour deposition of the simple monolayer coatings (K) and the chemical vapour deposition of multilayer coatings with the number of layers of $n<10$ (O) was classified as the least promising technologies with both, limited potential and attractiveness, hence placed in the least promising quarter of the matrix called a quaking aspen.

Table 2. *The results of studies into the structure and properties of sintered tool materials with the PVD and CVD coatings deposited*

Process	Coating	Substrate	Thic-kness, µm	Rough-ness R_a, µm	Hard-ness, HV	Hard-ness, ΔHV, %	Adhe-rence, L_c, N	Cutting para-meters	Tool life, min	Δ Tool life in-crease, %	Machi-ning quality, R_a, µm	Appli-cation (ISO 513)
(K) Simple monolayer coatings												
PVD monolayer	TiN	Cemented carbides	2.0	0.59	2000	11	50	D	8	533	2.4	P10-P35
PVD monolayer	TiN	Al_2O_3+ZrO$_2$	0.8	0.37	2240	22	45	A	11	0	2.4	K01
PVD monolayer	TiN	Al_2O_3+TiC	1.2	0.21	3330	72	47	A	18	33	1.4	K01, H05,
PVD monolayer	TiN	Al_2O_3+SiC$_{(w)}$	0.9	0.30	2760	50	38	B	10	19	1.9	S15, H10
PVD monolayer	TiN	Si_3N_4	0.8	0.34	2255	19.5	20	C	8	0	2.5	K10-K20
(L) Complex, classical monolayer coatings												
PVD monolayer	Ti(C,N)	Cemented carbides	4.0	0.55	2250	18	54	D	17	425	2,1	P25-P45
PVD monolayer	(Ti,Al)N	Al_2O_3+ZrO$_2$	2.2	0.23	3260	78	82	A	16	45	1.2	K01
PVD monolayer	(Ti,Al)N	Al_2O_3+TiC	2.2	0.07	3580	85	80	A	20	44	1.4	K01, H05,
PVD monolayer	(Ti,Al)N	Al_2O_3+SiC$_{(w)}$	2.8	0.26	3340	82	99	B	11	38	2.4	S15, H10
(M) Complex, nanocrystalline monolayer coatings												
PVD monolayer	(Ti,Al)N	Cemented carbides	2.2	0.14	2755	57	52	F	20	700	1.4	P25-P45
PVD monolayer	Ti(C,N)	Cemented carbides	1.5	0.13	2602	48	44	F	5	100	1.9	P25-P45
PVD monolayer	(Ti,Al)N	Cermet (A)	1.5	0.13	2900	57	54	F	20	680	1.3	P05-P35
PVD monolayer	Ti(C,N)	Cermet (A)	1.5	0.12	2950	59	42	F	8	220	2.0	P05-P35
PVD monolayer	(Ti,Al)N	Al_2O_3+TiC	1.6	0.27	3170	50	53	F	21	68	1.6	K01, H05,
PVD monolayer	Ti(C,N)	Al_2O_3+TiC	1.3	0.23	2850	35	41	F	15	20	1.8	K01, H05,
(N) PVD multilayer coatings, number of layers n<10												
PVD multilayer	TiN+(Ti,Al,Si)N	Cemented carbides	3.5	0.65	3100	72	57	D	20	2000	1.8	P10-P25
PVD multilayer	TiN+(Ti,Al,Si)N	Cemented carbides	3.5	0.64	3190	67	77	D	22	550	1.1	P10-P30
PVD multilayer	TiN+(Ti,Al,Si)N	Cermet (A)	3.5	0.62	3330	33	115	D	43	307	1.3	P05-P25
PVD multilayer	TiN+(Ti,Al,Si)N	Cermet (B)	3.5	0.60	3310	35	131	D	55	323	1.4	P05-P35
PVD multilayer	TiN+TiC+TiN	Cermet (A)	5.0	0,79	3000	20	79	D	35	250	1.5	P10-P40
PVD multilayer	TiN+(Ti,Al,Si)N	Al_2O_3+ZrO$_2$	1.9	0.43	1900	4	40	A	15	36	1.7	K01
PVD multilayer	TiN+(Ti,Al,Si)N	Al_2O_3+TiC	1.8	0.37	2510	30	40	A	18	30	1.6	K01, H05,
PVD multilayer	TiN+(Ti,Al,Si)N	Al_2O_3+SiC$_{(w)}$	2.5	0.37	2460	34	70	B	11	31	1.4	S15, H10

Process	Coating	Substrate	Thic-kness, μm	Rough-ness R_a, μm	Hard-ness, HV	Hard-ness, ΔHV, %	Adhe-rence, L_c, N	Cutting para-meters	Tool life, min	Δ Tool life in-crease, %	Machi-ning quality, R_a, μm	Appli-cation (ISO 513)
PVD multilayer	TiN+(Ti,Al,Si)N	Si_3N_4	2.0	0.45	2378	26	22	C	8	0	5.1	K10-K20
(O) CVD multilayer coatings, number of layers n<10												
CVD double	TiN+TiC/TiN	Cemented carbides	5.0	0.53	2400	26	57	D	21	525	1.8	P20-P35
CVD multilayer	Ti(C,N)+Al_2O_3+	Cemented carbides	12.5	0.51	2590	36	52	D	19	475	2.1	P10-P35
CVD multilayer	Ti(C,N)+Al_2O_3+	Cemented carbides	8.0	0.60	2300	21	78	D	23	575	2.1	P05-P30
CVD multilayer	Ti(C,N)+	Cemented carbides	8.4	0.63	2315	27	93	E	23	1050	3.7	S05-S15
CVD multilayer	Ti(C,N)+TiN	Cemented carbides	5.0	0.40	2443	34	110	E	27	1250	4.4	S05-S15
CVD multilayer	Ti(C,N)+TiN	Al_2O_3+ZrO_2	1.5	0.25	2030	10	62	A	13	18	1.9	K01
CVD multilayer	TiN+Al_2O_3	Al_2O_3+ZrO_2	6.0	0.40	3380	84	73	A	17	54	1.9	K01
CVD multilayer	Ti(C,N)+TiN	Al_2O_3+TiC	1.1	0.07	2070	5	15	A	17	22	1.7	K01, H05,
CVD multilayer	TiN+Al_2O_3	Al_2O_3+TiC	5.8	0.29	3440	78	17	A	17	22	1.6	K01, H05,
CVD multilayer	Ti(C,N)+TiN	Al_2O_3+$SiC_{(w)}$	2.6	0.25	2250	22	40	B	9	6	1.8	S15, H10
CVD multilayer	TiN+Al_2O_3	Al_2O_3+$SiC_{(w)}$	7.9	0.30	3640	98	18	B	16	100	2.2	S15, H10
CVD multilayer	Ti(C,N)+TiN	Si_3N_4	4.2	0.15	2268	20.2	52	C	8	0	4.8	K10-K20
CVD multilayer	Ti(C,N)+Al_2O_3+	Si_3N_4	9.5	0.28	2050	9	27	C	8	0	4.6	K10-K20
CVD multilayer	TiC+TiN	Si_3N_4	5.4	0.25	2020	7	67	C	10	25	4.3	K10-K20
CVD multilayer	TiC+Ti(C,N)+Al	Si_3N_4	7.8	0.27	3025	60	32	C	8	0	5.0	K10-K20
CVD multilayer	TiN+Al_2O_3	Si_3N_4	10.0	0.45	3320	76	83	C	16	100	2.3	K10-K20
CVD multilayer	TiN+Al_2O_3+TiN	Si_3N_4	3.8	0.13	2487	31.9	48	C	15	88	3.7	K10-K20
CVD multilayer	Al_2O_3+TiN (1)	Si_3N_4	2.6	0.25	2676	41.9	45	C	16	100	3.8	K10-K20
CVD multilayer	Al_2O_3+TiN (2)	Si_3N_4	1.7	0.23	2775	47.9	27	C	14	75	2.7	K10-K20
CVD multilayer	TiN+Al_2O_3+TiN	Si_3N_4	4.5	0.60	2571	36.3	41	C	20	150	2.6	K10-K20
CVD multilayer	Ti(C,N)+	Sialon ceramics	7.0	0.82	2669	31	43	E	10	0	2.8	S05-S15
CVD multilayer	Ti(C,N)+TiN	Sialon ceramics	2.8	0.20	2746	35	72	E	15	50	2.1	S05-S15
(P) Multilayer coatings, number of layers n≥10												
PVD multilayer	TiN+multi(Ti,Al,	Cemented carbides	4.5	0.67	3200	77	60	D	27	2700	1.1	P10-P25
PVD multilayer	TiN+multi(Ti,Al,	Cemented carbides	4.5	0.66	3280	72	90	D	33	825	1.0	P10-P30
PVD multilayer	TiN+multi(Ti,Al,	Cermet (A)	4.5	0.63	3520	40	106	D	43	307	0.7	P05-P25

Process	Coating	Substrate	Thic-kness, µm	Rough-ness R_a, µm	Hard-ness, HV	Hard-ness, ΔHV, %	Adhe-rence, L_c, N	Cutting para-meters	Tool life, min	Δ Tool life in-crease, %	Machi-ning quality, R_a, µm	Appli-cation (ISO 513)
PVD multilayer	TiN+multi(Ti,Al,	Cermet (B)	4.5	0.62	3390	38	120	D	60	352	0.8	P05-P35
PVD multilayer	TiN+multi(Ti,Al,	Al_2O_3+ZrO$_2$	2.3	0.37	4050	121	76	A	14	27	1.8	K01
PVD multilayer	TiN+multi(Ti,Al,	Al_2O_3+TiC	1.5	0.27	3980	105	71	A	19	42	1.4	K01, H05,
PVD multilayer	TiN+multi(Ti,Al,	Al_2O_3+SiC$_{(w)}$	2.8	0.33	3970	116	58	B	11	38	1.1	S15, H10
PVD multilayer	TiN+multi(Ti,Al,	Si_3N_4	4.0	0.44	3592	91	52	C	10	25	4.1	K10-K20
PVD multi	multi(Al,Cr)N	Cemented carbides	3.8	0.28	2867	57	96	E	45	2150	4.9	S05-S15
PVD multi	muti(Al, Cr)N	Sialon ceramics	4.8	0.31	2230	10	53	E	50	400	3.2	S05-S15
(R) Step-graded coatings												
PVD graded,	Ti(C,N) +	Cemented carbides	2.8	0.31	3076	68	39	E	15	650	4.0	S05-S15
PVD graded	TiN+(Ti,Al,Si)N	Al_2O_3+ZrO$_2$	2.2	0.40	2060	12	78	A	16	45	1.2	K01
PVD graded	TiN+(Ti,Al,Si)N	Al_2O_3+TiC	2.0	0.24	3040	57	77	A	16	19	2.0	K01, H05,
PVD graded	TiN+(Ti,Al,Si)N	Al_2O_3+SiC$_{(w)}$	2.5	0.32	2370	29	80	B	11	31	1.4	S15, H10
PVD multilayer	TiN+(Ti,Al,Si)N	Si_3N_4	2.5	0.32	2731	44.8	18	C	9	13	5.7	K10-K20
PVD graded,	Ti(C,N) +	Sialon ceramics	1.4	0.30	2786	37	36	E	10	0	2.2	S05-S15
(S) Continuous graded coatings												
PVD graded	Ti(C,N)	Cemented carbides (B)	2.7	0.11	2850	62	64	F	6	140	3.2	P25-P45
PVD graded	(Ti,Al)N	Cemented carbides (B)	2.6	0.14	3000	70	56	F	26	920	3.5	P25-P45
PVD graded	Ti(B,N)	Cemented carbides (A)	1.8	0.29	2951	62	34	E	15	650	4.0	S10-S15
PVD graded	(Ti,Zr)N	Cemented carbides (A)	3.0	0.30	2842	56	40	E	13	550	3.8	S05-S15
PVD graded	Ti(C,N) (1)	Cemented carbides	2.1	0.22	2871	57	49	E	13	550	4.5	S05-S15
PVD graded	Ti(C,N) (2)	Cemented carbides	2.1	0.32	3101	70	77	E	53	2550	4.2	S05-S15
PVD graded	(Al,Ti)N	Cemented carbides	2.5	0.18	3301	81	100	E	55	2650	3.9	S05-S15
PVD graded	(Ti,Al)N	Cemented carbides	3.5	0.39	3327	82	109	E	60	2900	3.5	S05-S15
PVD graded	(Ti,Al)N	Cermet (A)	3.0	0.12	3150	70	63	F	22	780	3.1	P05-P35
PVD graded	Ti(C,N)	Cermet (A)	2.6	0.11	2951	59	60	F	10	280	3.3	P05-P35

Process	Coating	Substrate	Thic-kness, µm	Rough-ness R_a, µm	Hard-ness, HV	Hard-ness, ΔHV, %	Adhe-rence, L_c, N	Cutting para-meters	Tool life, min	Δ Tool life in-crease, %	Machi-ning quality, R_a, µm	Appli-cation (ISO 513)
PVD graded	(Ti,Al)N	Al_2O_3+Ti C	3.2	0.24	3201	52	65	F	40	220	2.8	K01, H05,
PVD graded	Ti(C,N)	Al_2O_3+Ti C	2.1	0.21	2951	40	55	F	19	52	2.4	K01, H05,
PVD graded	Ti(B,N)	Sialon ceramics	1.3	0.25	2676	31	13	E	10	0	2.2	S05-S15
PVD graded	(Ti,Zr)N	Sialon ceramics	2.3	0.40	2916	43	21	E	11	10	2.0	S05-S15
PVD graded	Ti(C,N) (1)	Sialon ceramics	1.5	0.23	2872	41	25	E	10	0	2.1	S05-S15
PVD graded	Ti(C,N) (2)	Sialon ceramics	1.8	0.38	2843	40	26	E	12	20	2.3	S05-S15
PVD graded	(Al,Ti)N	Sialon ceramics	3.0	0.15	3600	77	112	E	72	620	2.2	S05-S15
PVD graded	(Ti,Al)N	Sialon ceramics	5.0	0.28	2961	46	21	E	12	20	2.1	S05-S15

LEGEND:

Abbreviation	Detail marked substrate kind	Phase composition
Cemented carbides (A)	A-type cemented carbides	WC, Co
Cemented carbides (B)	B-type cemented carbides	WC, TiC, TaC, Co
Cermet (A)	A-type cermet	Ti(C,N), WC, TiC, TaC, Co, Ni
Cermet (B)	B-type cermet	Ti(C,N), TiC, TaC, WC, Co, Ni

Cutting parameters:

A – feed of f = 0.15 mm per rev., rolling depth of a_p = 2 mm, cutting speed of v_c = 200 m/min, machined material: grey cast iron

B – feed of f = 0.2 mm per rev., rolling depth of a_p = 2 mm, cutting speed of v_c = 250 m/min, machined material: ductile cast iron

C – feed of f = 0.2 mm per rev., rolling depth of a_p = 2 mm, cutting speed of v_c = 400 m/min. , machined material: grey cast iron EN-GJL-250

D -feed of f = 0.1 mm per rev., rolling depth of a_p = 1 mm, cutting speed of v_c = 250; 315; 400 m/min., non-alloy steel C45E

E – feed of f = 0.2 mm per rev., rolling depth of a_p = 1 mm, cutting speed of v_c = 180 m/min, machined material: grey cast iron

F – feed of f = 0.1 mm per rev., rolling depth of a_p = 1 mm, cutting speed of v_c = 150 m/min, machined material: e.g. grey cast iron

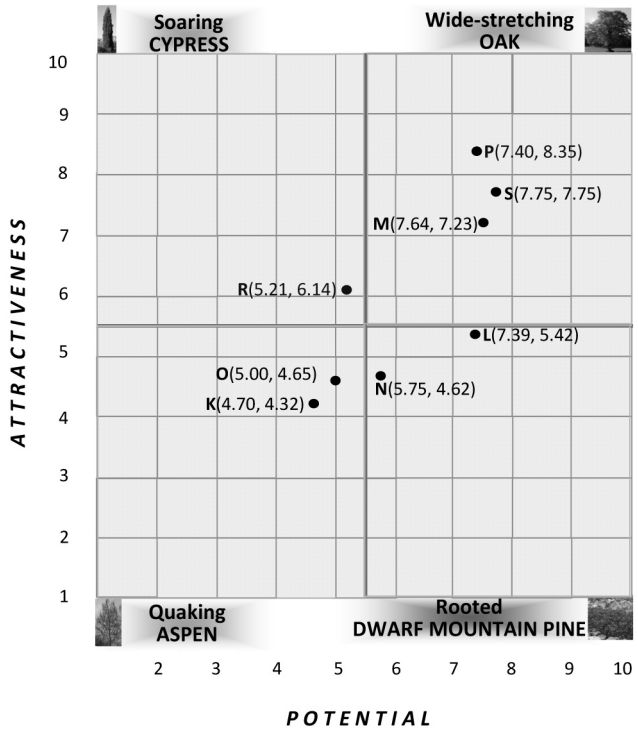

***Figure 32**. The dendrological matrix of technology value prepared for the (K)-(S) physical/chemical vapour deposition onto sintered tool materials*

The positive and negative environment influence on the relevant groups of technologies was evaluated with the meteorological matrix of environment influence. Entered into the matrix were the results of the multi-criteria analysis of the rates acquired when surveying the experts, see Fig. 33. The results of the investigations conducted show that the environment conditions are most supportive to the development of the physical vapour deposition of the continuous graded coatings (S), multilayer coatings with the number of layers of $n \geq 10$ (P) and complex, nanocrystalline monolayer coatings (M) included in the most promising quarter of the matrix called sunny spring. The macro- and micro-environment of such technologies is characterised by few difficulties and numerous opportunities which should help in their further rapid development. The environment for the other investigated groups of technologies is predictable and stable with a neutral character, therefore, no related spectacular opportunities should be expected from it, nor unpredictable difficulties which encourages regular, gradual progress.

At the next stage of research work, the results of the studies presented graphically with the dendrological matrix of technologies value and meteorological matrix environment influence were entered into the technologies strategy matrix (Fig. 34). The matrix is presenting, graphically, the place of the tested physical and chemical vapour deposition technologies onto sintered tool materials according to their value and environment influence intensity, indicating the relevant managing strategy.

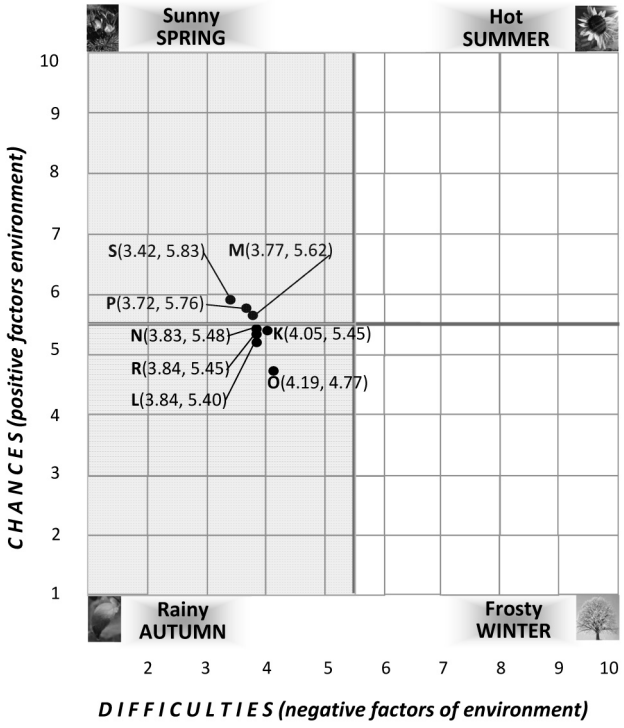

***Figure 33**. Meteorological matrix of environment influence prepared for the (K)-(S) physical/chemical vapour deposition onto sintered tool materials*

Using pre-defined mathematical relationships, the specific numerical values provided in the dendrological and meteorological matrix dimensioned [2x2] were moved to the strategy matrix for technologies dimensioned [4x4]. The circles mark the strategic development prospects of a given group of technologies expressed in numbers.

As regards (P), (S) and (M) technologies awarded 9 points in a ten-degree scale, it is recommended to use an oak in spring strategy guaranteeing the future success related to

developing, strengthening and implementing an attractive technology with a large potential in favourable environment conditions. The multilayer coatings with the number of layers of $n \geq 10$ (P), continuous graded coatings (S) and complex, nanocrystalline monolayer coatings (M) deposited in the PVD process onto sintered tool materials are characterised by high microhardness limiting mechanical wear, by good adherence and a large relative tool life increase. Very good functional properties achieved as a result of applying the technology (P) encompassing both, the average values of mechanical properties as well as the best average tool life increase versus a material without the coating are most certainly connected with the using the systems of nanolayers. They allow to differentiate very well the properties in the individual zones of the coating and due to the structure designed in such a way, enable the very good adherence of individual nanolayers and the coating's adherence to the substrate material [19-21]. The technology (S) ensuring a continuous gradient of the structure and of chemical composition, achieved through the continuous change of the concentration of the individual elements forming part of the coating material of the coating surface towards the substrate also allow to achieve good mechanical and functional properties. The continuous gradient applied causes the better relaxation of internal stresses occurring in the coating and eliminates an issue of mutual adherence for individual layers existing in case of the step-graded coatings. [23,69]. The monolayer, complex nanocrystalline coatings deposited in the PVD (M) process are also characterised by very good mechanical properties translating into a high relative increase in tool life accomplished during a technological cutting test. They are also characterised by relatively the lowest roughness.

A strategy of a dwarf mountain pine in autumn recommended for the technologies (L) and (N) assumes that profits are derived from running production in a stable, predictable environment using a solid technology that should be modernised and intensively promoted to improve its attractiveness. The technology (L) evaluated most highly in this group, implemented into sintered tool materials, received 7 out of 10 available points, ensures hard coatings with excellent adherence leading to the highest average tool life characterised for such materials. Very high adherence achieved for materials with the classical, complex coatings deposited may be related to the advantageously selected substrate and coating type combinations resulting in stresses being distributed more advantageously in the zone between the substrate and coating in this group of materials. Development prospects for the technology (N) were found to be moderate (6 points). This reflects the slightly worse properties of the sintered tool materials coated with the multi-layer coatings with the number of layers of $n<10$

(N) as compared to the monolayer, classical, complex coatings (L). The technology (R): physical vapour deposition of the step-graded coatings also offers moderate development prospects (6 points) and for its the cypress in autumn strategy is recommended. The strategy consists in using a stable, predictable environment for production using an attractive technology while strengthening its potential. The issue of mutual adherence of the individual layers of the step-graded coatings needs to be solved in particular.

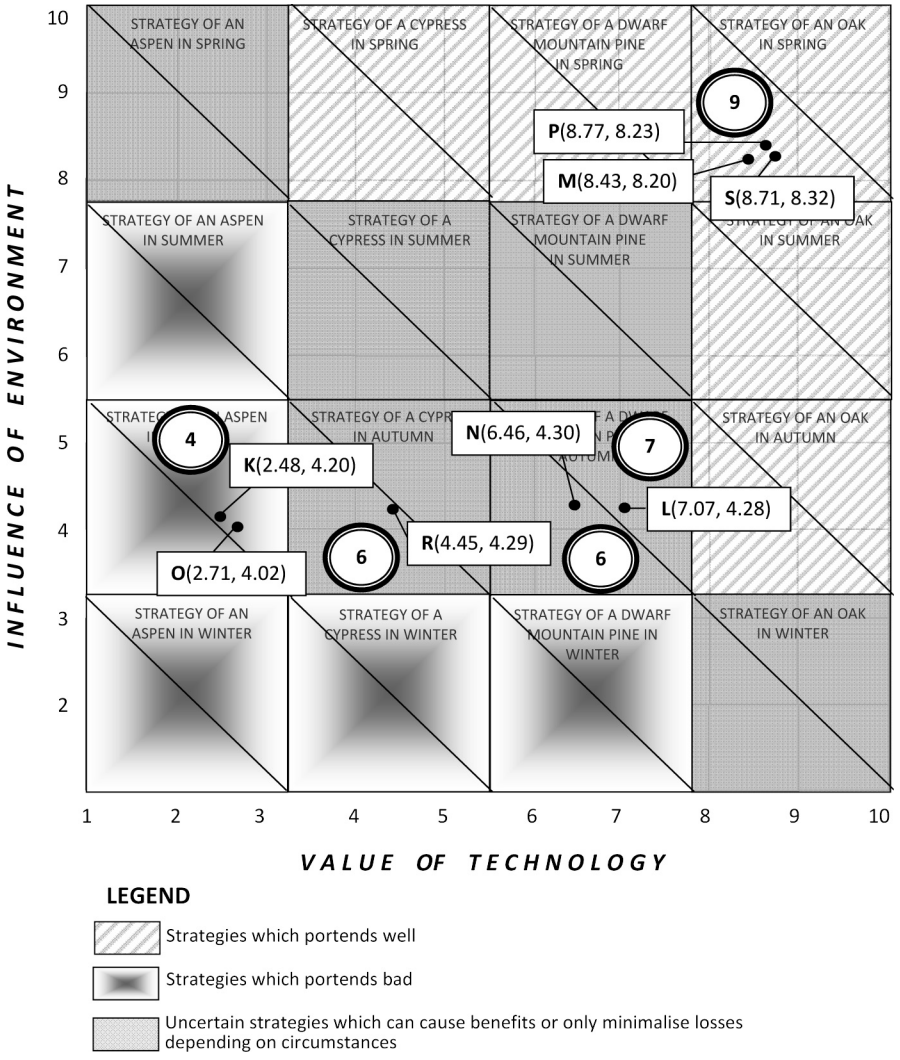

***Figure 34**. The matrix of strategies for technologies prepared for prepared for the (K)-(S) physical/chemical vapour deposition onto sintered tool materials*

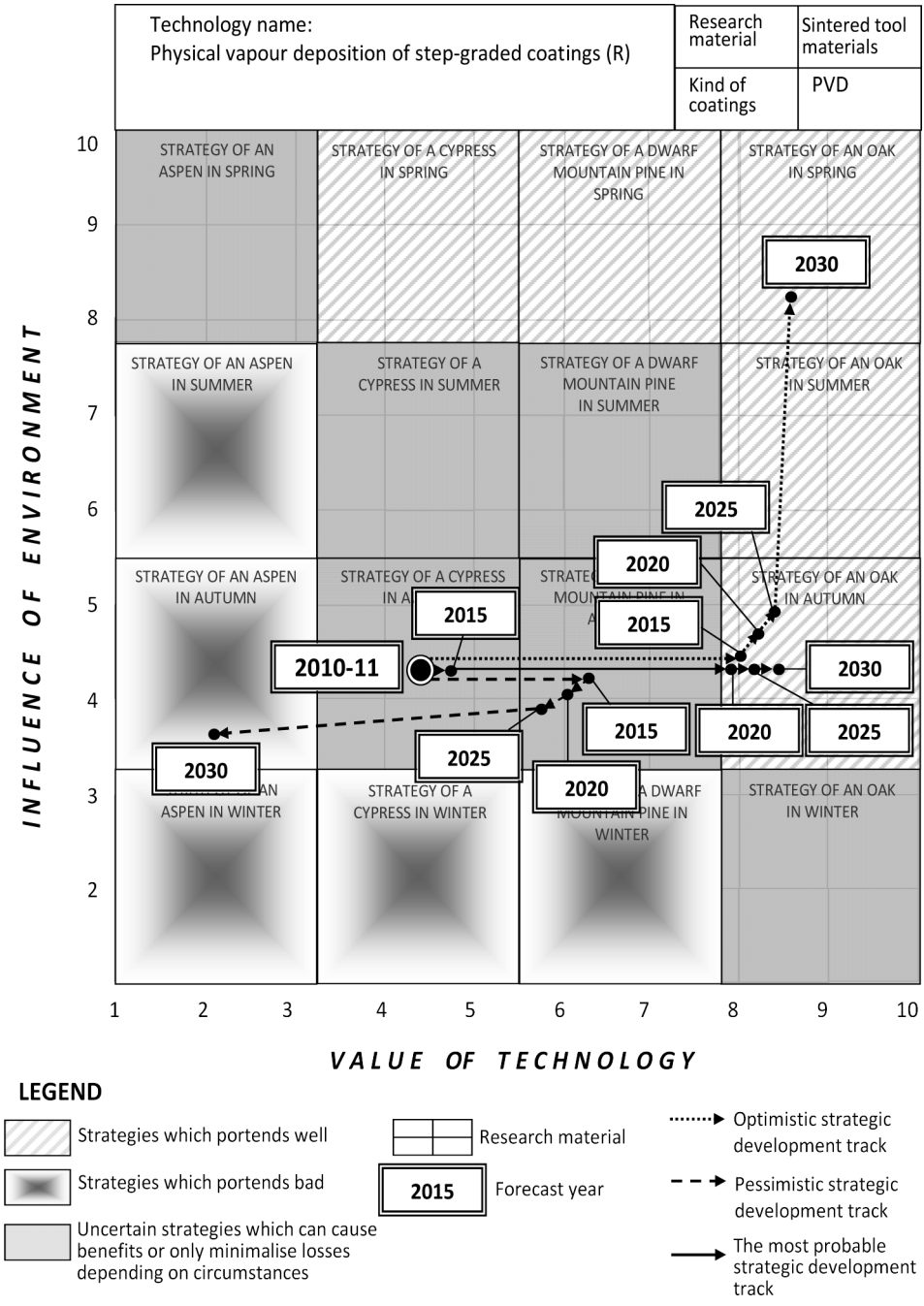

***Figure 35**. The strategic development tracks created for the (R) demonstration technology: the physical vapour deposition of the step-graded coatings*

The physical vapour deposition of the simple monolayer coatings (K) and the chemical vapour deposition of the multilayer coatings with the number of layers of $n<10$ (O) were found out in the group of technologies featuring the weakest development prospects with their value assessed quite low (4) in the ten-degree scale. It is predicted that in the long-term horizon, the value of such technologies will still be weakening and they will be slowly replaced with ones allowing to deposited coatings with better mechanical and functional properties.

Strategic development tracks for the individual technology groups were established based on the acquired expert opinions. The tracks represent an optimistic, most probable and pessimistic forecast of their development for the relevant time intervals of 2015, 2020, 2025 and 2030. A future success is guarantee for the technologies (P), (S) and (M). It is anticipated that they will be widely used in the nearest 20 years for manufacturing hard tools, especially cutting tools for machining metallic, non-ferrous and hard-to-machine materials for the aviation, automotive and military industry as well as for civil engineering. The macro-environmental factors, especially the overall condition of the global economy will be conditioning the rate of the forecast progress. The technologies (L) and (N) will develop at a somewhat slower rate and the rate of their future success will depend on the range of their individual, specific applications. The future strategic position of the technology (R) will depend on the advancement of works aimed at strengthening their potential. In the optimistic scenario, the technologies may be found out in the best field of the matrix in the future (oak in summer), and in the pessimistic scenario, they may be completely degraded out and forced out by more attractive technologies. The least promising technologies are (K) and (O) and if a sudden breakthrough in their development is not seen through finding new industrial uses, the technologies will most probably be backed out from the market in the nearest 20 years. A graphical example of the strategy matrix for the technologies with strategic development tracks provided in three variants created for the physical vapour deposition of the step-graded coatings (R) is depicted in Fig. 35.

5. Technology Roadmapping

On the basis of the results of the foresight–materials science research concerning critical technologies the Critical Technologies Book including technology roadmaps [80-82] and

technology information sheets has been prepared (Fig. 36). The set-up of the custom technology roadmap corresponds to the first quarter of the Cartesian system of coordinates. Three time intervals for the years of: 2010-11 (current situation), 2020 (goals fulfilment methods), 2030 (long-term objectives) are provided on the axis of abscissa. A time horizon for the overall foresight research pursued with its results applied onto the map is 20 years. Seven main layers were applied onto the axis of coordinates of the technology roadmap: time layer, concept layer, product layer, technology layer, spatial layer, staff layer and quantitative layer, made up of more detailed sub-layers. The main technology roadmap layers were hierarchised starting with the top, most general layers determining all-social and economic reasons and causes of the actions taken, through the middle layers characterising a product and its manufacturing technology, to the bottom layers detailing organisational and technical matters concerning the place, contractor and costs.

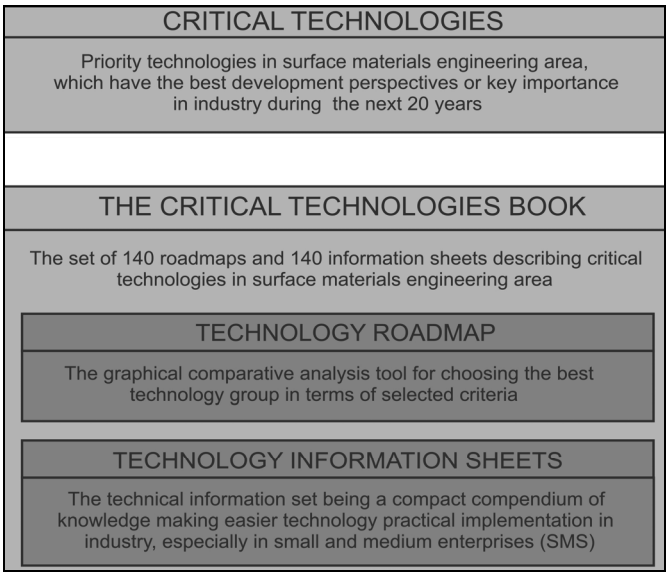

***Figure 36**. The Critical Technologies Book content*

The relationships between the individual layers and sub-layers of the technology roadmap are presented with the different types of arrows representing, respectively, cause and effect relationships, capital ties, time correlations and two-directional data and/or resources flow.

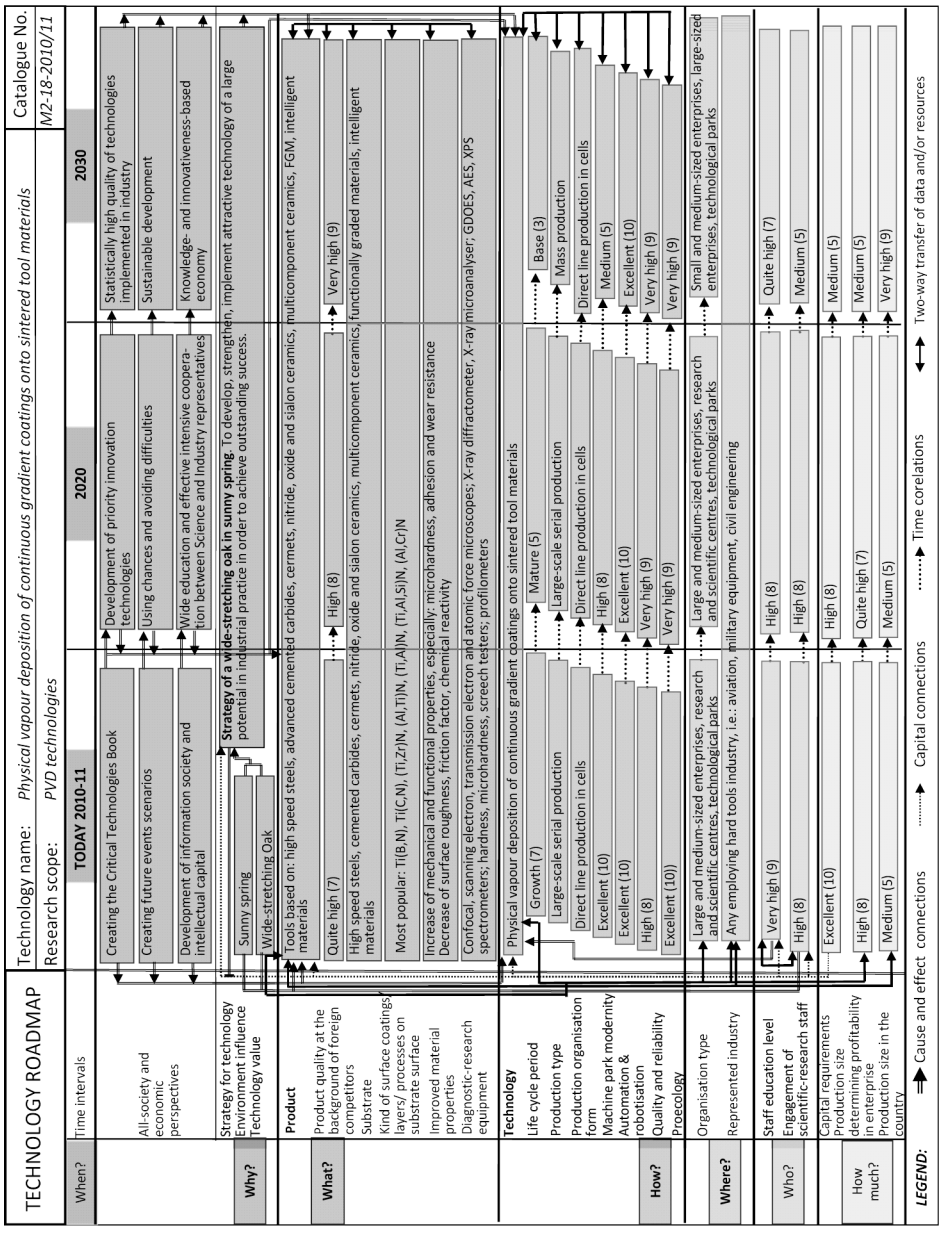

***Figure 37**. An example technology roadmap made for the physical vapour deposition of the continuous gradient coatings onto sintered tool materials*

Table 3. *Selected main source data used for preparation of technology roadmaps for investigated sintered tool materials with deposited coatings*

Technology symbol	Analysed factors																							
	(1)			(2)			(3)			(4)			(5)			(6)			(7)			(8)		
	Time horizon																							
	a	b	c	a	b	c	a	b	c	a	b	c	a	b	c	a	b	c	a	b	c	a	b	c
(K)	6	3	1	9	7	3	7	7	6	10	9	9	8	7	5	8	6	4	8	6	4	6	5	5
(L)	7	5	3	10	8	5	8	9	9	10	9	9	9	7	5	9	7	5	8	7	5	6	7	8
(M)	7	5	3	10	8	5	8	9	9	10	9	9	9	8	7	10	8	5	8	7	5	5	5	8
(N)	7	4	2	9	7	4	9	8	7	9	8	7	9	8	7	10	8	5	8	7	5	6	7	6
(O)	7	4	2	9	7	4	8	9	9	10	9	9	9	8	7	9	7	4	8	7	5	3	4	5
(P)	7	5	3	10	8	5	8	9	9	10	9	9	9	8	7	10	8	5	8	7	5	3	4	5
(R)	7	5	3	9	6	5	8	9	9	10	9	9	9	7	6	10	8	5	8	7	5	4	5	7
(S)	7	5	3	10	8	5	8	9	9	10	9	9	9	8	7	10	8	5	8	7	5	5	5	8

LEGEND

Technology symbol

(K) The physical vapour deposition of the simple monolayer coatings
(L) The physical vapour deposition of the complex, classical monolayer coatings
(M) The physical vapour deposition of the complex, nanocrystalline monolayer coatings
(N) The physical vapour deposition of the multilayer coatings, number of layers $n<10$
(O) The physical vapour deposition of the multilayer coatings, number of layers $n<10$
(P) The physical vapour deposition of the multilayer coatings, number of layers $n\geq10$
(R) The physical vapour deposition of the step-graded coatings
(S) The physical vapour deposition of the continuous graded coatings

Analysed factors

(1) Live cycle period
(2) Machine park modernity
(3) Quality and reliability
(4) Proecology
(5) Staff education level
(6) Capital requirements
(7) Production size determining profitability in enterprise
(8) Production size in the country

Time horizon

a: 2010-11 years
b: 2020 year
c: 2030 year

Note: Research results are presented in universal scale of relative state, where:1 is minimal and 10 is excellent level.

Fig. 37 provides a representative technology roadmap prepared for the physical vapour deposition of the continuous graded coatings (S), whereas Table 3 presents an aggregate list containing selected data being an extract from all the technology roadmaps developed under this chapter concerning sintered tool materials with the PVD/CVD coatings deposited. Technology information cards containing technical information very helpful in implementing a specific technology in the industrial practice, especially in small- and medium-size enterprises (SMEs) not having the capital allowing to conduct own research in this field, are detailing and supplementing the technology roadmaps.

6. Summary

This work presents the results of interdisciplinary, experimental and comparative research over sintered tool materials based on cemented carbides, cermets, oxide and nitride ceramics and sialon coated with hard layers coatings in the physical/ chemical vapour deposition processes. Eight homogenous groups of technologies (K)-(S) have been distinguished between for the purpose of the research by adopting physical or chemical vapour deposition onto sintered tool materials as a criterion of grouping. The materials science part of the work included in particular investigations into the structure of sintered tool materials, tests of structure, chemical composition and the phase composition of coatings and the testing of mechanical and functional properties of coatings. A comparative analysis was made for the results of the investigations, with special consideration given to roughness, microhardness, adherence of coatings and tool life increase relative to the material without a coating deposited during a technological cutting tests. A strategic position of the PVD and CVD strategies for the materials surface engineering was identified for foresight research along with a value against the environment of the individual, separated groups of physical and chemical vapour deposition technologies for sintered tool materials (K)-(S). The results of the investigations are presented graphically using a set of matrices. The long-term strategies recommended for implementation with regard to the individual, separate technologies are also presented. Technology roadmaps were prepared at the final stage of works illustrating, in a concise manner, basic information on the technologies analysed. The analysis made has shown that the physical vapour deposition of the multilayer coatings with the number of layers of $n \geq 10$ (P), continuous graded coatings (S) and complex, nanocrystalline monolayer coatings (M) with

their success being certain have the best long-term prospects. It is predicted that they will be widely used in the nearest 20 years for producing hard tools, especially cutting tools for machining metallic, non-ferrous and hard-to-machine materials for the aviation, automotive, military industry and for civil engineering. Somewhat slower but regular growth of the physical vapour deposition of the complex, classical monolayer coatings (L), the multilayer coatings with the number of layers of $n<10$ (N) and the step-graded coatings (R) is foreseen, depending on the environment conditions and the individual, specialised uses of such technologies. The least promising technologies include the physical vapour deposition of the simple monolayer coatings (K) and the chemical vapour deposition of the multilayer coatings with the number of layers of $n<10$ (O) to be forced out by other technologies allowing to achieve better mechanical and functional properties. When evaluating the importance of the state-of-art hard abrasive wear coatings deposited in PVD/CVD processes onto sintered tool materials presented in the chapter, their broad scale of future applications in the industry should be emphasised. Hence, they will be very important in the nearest 20 years amongst other technologies of engineer materials surface engineering, which justifies their position in The Critical Technologies Book.

References

1. FutMan. The Future of Manufacturing in Europe 2015-2020; The Challenge for Sustainability; Materials; Final Report; Groupe CM International, 2003, http://ec.europa. eu/research/-industrialtechnologies/pdf/pro-futman-doc3a. pdf.
2. MatVis. C. Dreher, Manufacturing visions: A holistic view of the trends for European manufacturing, in: M. Montorio, M. Taisch, K.-D. Thoben (eds.), Advanced Manufacturing. An ICT and Systems Perspective, Taylor & Francis Group, London, 2007.
3. H Dosch, M.H. Van de Voorde (eds.), Gennesys. White Paper. A New European Partnership between Nanomaterials Science & Nanotechnology and Synchrotron Radiation and Neuron Facilities, Max-Planck-Insititut für Metalforschung, Stuttgart, 2009.
4. NANOMAT, Headed by A. Szajdak, www.nanomat.eitplus.pl.
5. Technology foresight of polymeric materials in Poland, K. Czaplicka-Kolarz (ed.), Steady state analysis, Totem Publisher, Poznan, 2008 (in Polish).
6. Advanced Industrial and Ecological Technologies for Sustainable Development of Poland, Headed by A. Mazurkiewicz, www.portaltechnologii.pl/3index/index.html.

7. FORGOM, Headed by K. Czaplicka-Kolarz, J. Bondaruk, www.foresightgom.pl.
8. FOREMAT, Technology Development Scenarios of Modern Metallic, Ceramic and Composites Materials. Reports of Project Co-Operators, B. Gambin, W. Łojkowski, A. Świderska-Środa (eds.), Unipress Publisher, Radom, 2010 (in Polish).
9. L.A. Dobrzański, Forming the structure and surface properties of engineering and biomedical materials, Foresight of surface properties formation leading technologies of engineering materials and biomaterials. International OCSCO World Press, Gliwice 2009.
10. A.D. Dobrzańska-Danikiewicz, Computer Aided Foresight Integrated Research Methodology in Surface Engineering Area, work in progress.
11. A.D. Dobrzańska-Danikiewicz, Foresight methods for technology validation, roadmapping and development in the surface engineering area, Archives of Materials Science Engineering 44/2 (2010) 69-86.
12. A.D. Dobrzańska-Danikiewicz, E-foresight of materials surface engineering, Archives of Materials Science and Engineering 44/1 (2010) 43-50.
13. A.D. Dobrzańska-Danikiewicz, E. Jonda, K. Labisz, Foresight methods application for evaluating laser treatment of hot-work steels, Journal of Achievements in Materials and Manufacturing Engineering 43/2 (2010) 750-773.
14. A.D. Dobrzańska-Danikiewicz, T. Tański, S. Malara, J. Domagała-Dubiel, Assessment of strategic development perspectives of laser treatment of casting magnesium alloys, Archives of Materials Science Engineering 45/1 (2010) 5-39.
15. A.D. Dobrzańska-Danikiewicz, A. Drygała, Foresight methodology application for laser texturing of silicon surface, Proceedings of Polish-Ukrainian Scientific Conference - Mechanics and Computer Science, Chmielnicki, Ukraine, 2011, 156-157.
16. A.D. Dobrzańska-Danikiewicz, K. Lukaszkowicz, Technology validation of coatings deposition onto the brass substrate, Archives of Materials Science Engineering 46/1 (2010) 5-38.
17. A.D. Dobrzańska-Danikiewicz, A. Kloc-Ptaszna, B. Dołżańska, Determination of tool gradient materials value according to foresight methodology, Journal of Achievements in Materials and Manufacturing Engineering, article in press (2011).
18. A.D. Dobrzańska-Danikiewicz, E. Hajduczek, M. Polok-Rubiniec, M. Przybył, K. Adamaszek, Evaluation of selected steel thermochemical treatment technology using foresight methods, Journal of Achievements in Materials and Manufacturing Engineering, 46/2 (2011) 115-146.
19. L.A. Dobrzański, K. Gołombek, J. Kopač, M. Soković, Effect of depositing the hard surface coatings on properties of the selected cemented carbides and tool cermets, Journal of Materials Processing Technology 157-158 (2004) 304-311.
20. L.A. Dobrzański, J. Mikuła, The structure and functional properties of PVD and CVD coated Al_2O_3+ZrO_2 oxide tool ceramics, Journal of Materials Processing Technology 167 (2005) 438-446.

21. L.A. Dobrzański, D. Pakuła, Comparison of the structure and properties of the PVD and CVD coatings deposited on nitride tool ceramics, Journal of Materials Processing Technology 164-165 (2005) 832-842.
22. L.A. Dobrzański, D. Pakuła, E. Hajduczek, Structure and properties of the multi-component TiAlSiN coatings obtained in the PVD process in the nitride tool ceramics, Journal of Materials Processing Technology 157-158 (2004) 331-340.
23. L.A. Dobrzański, M. Staszuk, J. Konieczny, W. Kwaśny, M. Pawlyta, Structure of TiBN coatings deposited onto cemented carbides and sialon tool ceramics, Archives of Materials Science and Engineering 38/1 (2009) 48-54.
24. I.Yu. Konyashin, PVD/CVD technology for coating cemented carbides, Surface and Coatings Technology 71 (1995) 277-283.
25. P.H. Mayrhofer, C. Mitterer, L. Hultman, H. Clemens, Microstructural design of hard coatings, Progress in Materials Science 51 (2006) 1032-1114.
26. D. Pakuła, L.A. Dobrzański, A. Križ, M. Staszuk, Investigation of PVD coatings deposited on the Si3N4 and sialon tool ceramics, Archives of Materials Science and Engineering 46/1 (2010) 53-60.
27. M.A. Baker, P.J. Kench, C. Tsotsos, P.N. Gibson, A. Leyland, A. Matthews, Investigation of the nanostructure and wear properties of physical vapor deposited CrCuN nanocomposite coatings, Journal of Vacuum Science and Technology A 23/3 (2005) 423-433.
28. S. Veprek, M.G.J. Veprek-Heijman, The formation and role of interfaces in superhard nc-MenN/a-Si3N4 nanocomposites, Surface and Coatings Technology 201/13 (2007) 6064-6070.
29. A.A. Voevodin, T.A. Fitz, J.J. Hu, J.S. Zabinski, Nanocomposite tribological coatings with "chameleon" surface adaptation, Journal of Vacuum Science and Technology A 20/4 (2002) 1434-1444.
30. C.W. Zou, H.J. Wang, M. Li, Y.F. Yu, C.S. Liu, L.P. Guo, D.J. Fu, Characterization and properties of TiN-containing amorphous Ti–Si–N nanocomposite coatings prepared by arc assisted middle frequency magnetron sputtering, Vacuum 84 (2010) 817-822.
31. S.J. Bull, D.G. Bhat, M.H. Staia, Properties and performance of commercial TiCN coatings. Part 2: tribological performance, Surface and Coatings Technology 163-164 (2003) 507-514.
32. K. Chu, P.W. Shum, Y.G. Shen, Substrate bias effects on mechanical and tribological properties of substitutional solid solution (Ti, Al)N films prepared by reactive magnetron sputtering, Materials Science and Engineering B 131 (2006) 62-71.
33. L.A. Dobrzański, D. Pakuła, A. Křiž, M. Soković, J. Kopač, Tribological properties of the PVD and CVD coatings deposited onto the nitride tool ceramics, Journal of Materials Processing Technology 175 (2006) 179-185.
34. G.S. Fox-Rabinovich, K. Yamomoto, S.C. Veldhuis, A.I. Kovalev, G.K. Dosbaeva, Tribological adaptability of TiAlCrN PVD coatings under high performance dry machining conditions, Surface and Coatings Technology 200/5-6 (2005) 1804-1813.

35. I.W. Park, D.S. Kang, J.J. Moore, S.C. Kwon, J.J. Rha, K.H. Kim, Microstructures, mechanical properties, and tribological behaviors of Cr–Al–N, Cr–Si–N, and Cr–Al–Si–N coatings by a hybrid coating system, Surface and Coatings Technology 201/9-11 (2007) 5223-5227.
36. C. Rebholz, H. Ziegele, A. Leyland, A. Matthews, Structure, mechanical and tribological properties of Ti–B–N and Ti–Al–B–N multiphase thin films produced by electron-beam evaporation, Journal of Vacuum Science and Technology A 16/5 (1998) 2851-2857.
37. D.V. Shtansky, Ph.V. Kiryukhantsev-Korneev, I.A. Bashkova, A.N. Sheveiko, E.A. Levashov, Multicomponent nanostructured films for various tribological applications, International Journal of Refractory Metals and Hard Materials 28/1 (2010) 32-39.
38. R. Bayón, A. Igartua, X. Fernández, R. Martínez, R.J. Rodríguez, J.A. García, A. de Frutos, M.A. Arenas, J. de Damborenea, Corrosion wear behaviour of PVD Cr/CrN multilayer coatings for gear applications, Tribology International 42/4 (2009) 591-599.
39. A. Conde, C. Navas, A.B. Cristobal, J. Housden, J. de Damborenea, Characterisation of corrosion and wear behaviour of nanoscaled e-beam PVD CrN coatings, Surface and Coatings Technology 201/6 (2006) 2690-2695.
40. L.A. Dobrzański, K. Lukaszkowicz, A. Zarychta, L. Cunha, Corrosion resistance of multilayer coatings deposited by pvd techniques onto the brass substrate, Journal of Materials Processing Technology 164-165 (2005) 816-821.
41. M. Fenker, M. Balzer, H. Kappl, A. Savan, Corrosion behaviour of MoSx-based coatings deposited onto high speed steel by magnetron sputtering, Surface and Coatings Technology 201/7 (2006) 4099.
42. K. Lukaszkowicz, J. Sondor, A. Kriz, M. Pancielejko, Structure, mechanical properties and corrosion resistance of nanocomposite coatings deposited by PVD technology onto the X6CrNiMoTi17-12-2 and X40CrMoV5-1 steel substrates, Journal of Materials Science 45/6 (2010) 1629-1637.
43. A.A. Voevodin, J.S. Zabinski, Nanocomposite and nanostructured tribological materials for space applications, Composites Science and Technology 65/5 (2005) 741-748.
44. Y.C. Cheng, T. Browne, B. Heckerman, E.I. Meletis, Mechanical and tribological properties of nanocomposite TiSiN coatings, Surface and Coatings Technology 204/14 (2010) 2123-2129.
45. L.A. Dobrzański, K. Lukaszkowicz, Erosion resistance and tribological properties of coatings deposited by reactive magnetron sputtering method onto the brass substrate, Journal of Materials Processing Technology 157-158 (2004) 317-323.
46. S. Imamura, H. Fukui, A. Shibata, N. Omori, M. Setoyama, Properties and cutting performance of AlTiCrN/TiSiCN bilayer coatings deposited by cathodic-arc ion plating, Surface and Coatings Technology 202/4-7 (2007) 820-825.
47. W. Kwaśny, Predicting properties of PVD and CVD coatings based on fractal quantities describing their surface, Journal of Achievements in Materials and Manufacturing Engineering 37/2 (2009) 125-192.

48. C. Li, S.Q. Wang, D. Yong, J. Li, Microstructure and mechanical properties of gradient Ti(C,N) and TiN/Ti(C, N) multilayer PVD coatings, Materials Science and Engineering A 478 (2008) 336-339.
49. C.Y.H. Lim, S.C. Lim, K.S. Lee, Wear of TiC-coated carbide tools in dry turning, Wear 225-229 (1999) 354-367.
50. D. Pakuła, L.A. Dobrzański, K. Gołombek, M. Pancielejko, A. Kriź, Structure and properties of the Si3N4 nitride ceramics with hard wear resistant coatings, Journal of Materials Processing Technology 157-158 (2004) 388-393.
51. S. PalDey, S.C. Deevi, Single layer and multilayer wear resistant coatings of (Ti,Al)N: a review, Materials Science and Engineering A 342 (2003) 59-79.
52. M. Soković, M. Bahor, On the inter-relationships of some machinability parameters in finish machining with cermet TiN (PVD) coated tools, Journal of Materials Processing Technology 78/1-3 (1998) 163-170.
53. M. Soković, J. Kopač, L.A. Dobrzański, J. Mikuła, K. Gołombek, D. Pakuła, Cutting characteristics of PVD and CVD –coated ceramic tool inserts, Tribology in industry 28/1-2 (2006) 3-8.
54. V.V. Uglov, V.M. Anishchik, S.V. Zlotski, G. Abadias, S.N. Dub, Stress and mechanical properties of Ti–Cr–N gradient coatings deposited by vacuum arc, Surface and Coatings Technology 200 (2005) 178-181.
55. S. Veprek, M.J.G. Veprek-Heijman, Industrial applications of superhard nanocomposite coatings, Surface and Coatings Technology 202/21 (2008) 5063-5073.
56. S. Veprek, M.G.J. Veprek-Heijman, P. Karvankova, J. Prochazka, Different approaches to superhard coatings and nanocomposites, Thin Solid Films 476/1 (2005) 1-29.
57. J.L. Endrino, G.S. Fox-Rabinovich, A. Reiter, S.V. Veldhuis, R. Escobar Galino, J.M. Albela, J.F. Marco, Oxidation tuning in AlCrN coatings, Surface and Coatings Technology 201/8 (2007) 4505-4511.
58. P. Karvankova, M.G.J. Veprek-Heijman, M. Zawrah, S. Veprek, Thermal stability of nc-TiN/a-BN/a-TiB2 nanocomposite coatings deposited by plasma chemical vapor deposition, Thin Solid Films 467/1-2 (2004) 133-139.
59. M. Kawate, A.K. Hashimoto, T. Suzuki, Oxidation resistance of Cr1−XAlXN and Ti1−XAlXN films, Surface and Coatings Technology 165/2 (2003) 163-167.
60. D.B. Lee, T.D. Nguyen, S.K. Kim, Air-oxidation of nano-multilayered CrAlSiN thin films between 800 and 1000 °C, Surface and Coatings Technology 203/9 (2009) 1199-1204.
61. A.E. Reiter, V.H. Derflinger, B. Hasenmann, T. Bachmann, B. Sartory, Investigation of the properties of Al1−xCrxN coatings prepared by cathodic arc evaporation, Surface and Coatings Technology 200/7 (2005) 2114-2122.
62. L.A. Dobrzański, Structure and properties of high-speed steels with wear resistant cases or coatings, Journal of Materials Processing Technology 109 (2001) 44-51.
63. L.A. Dobrzański, M. Adamiak, Structure and properties of the TiN and Ti(C,N) coatings deposited in the PVD process on high-speed steels, Journal of Materials Processing Technology 133 (2003) 50-62.

64. L.A. Dobrzański, A. Zarychta, The structure and properties of W-Mo-V high-speed steels with increased contents of Si and Nb after heat treatment, Journal of Materials Processing Technology 77 (1998) 180-193.
65. L.A. Dobrzański, A. Zarychta, M. Ligarski, High-speed steels with addition of niobium or titanium, Journal of Materials Processing Technology 63 (1997) 531-541.
66. L.A. Dobrzański, A. Zarychta, M. Ligarski, Phase transformations during heat treatment of W-Mo-V 11-2-2 type high-speed steels with increased contents of Si and Nb or Ti, Journal of Materials Processing Technology 53 (1995) 109-120.
67. M. Pancielejko, W. Precht, Structure, chemical and phase composition of hard titanium carbon nitride coatings deposited on HS6-5-2 steel, Journal of Materials Processing Technology 157-158 (2004) 394-298.
68. M. Soković, J. Kopač, L.A. Dobrzański, M. Adamiak, Wear of PVD-coated solid carbide end mills in dry high-speed cutting, Journal of Materials Processing Technology 157-158 (2004) 422-426.
69. L.A. Dobrzański, M. Staszuk, K. Gołombek, A. Śliwa, M. Pancielejko, Structure and properties PVD and CVD coatings deposited onto edges of sintered cutting tools, Archives of Metallurgy and Materials 55/1 (2010) 187-193.
70. L.A. Dobrzański, Design and manufacturing functional gradient tool materials – dependence properties on technology and thickness of surface layers with a gradient of both chemical and phase composition manufactured on tool from different applications. Design and manufacturing functional gradient materials, The Polish Academy of Science, Cracow 2007.
71. L.A. Dobrzański, K. Gołombek, Structure and properties of the cutting tools made from cemented carbides and cermets with the TiN + mono-, gradient- or multi(Ti,Al,Si)N + TiN nanocrystalline coatings, Journal of Materials Processing Technology 164-165 (2005) 805-815.
72. L.A. Dobrzański, K. Gołombek, E. Hajduczek, Structure of the nanocrystalline coatings obtained on the CAE process on the sintered tool materials, Journal of Materials Processing Technology 175 (2006) 157-162.
73. Y.Y. Tse, D. Babonneau, A. Michel, G. Abadias, Nanometer-scale multilayer coatings combining a soft metallic phase and a hard nitride phase: study of the interface structure and morphology, Surface and Coating Technology 180-181 (2004) 470-477.
74. L.A. Dobrzański, K. Gołombek, J. Mikuła, D. Pakuła, Multilayer and gradient PVD coatings on the sintered tool materials, Journal of Achievements in Materials and Manufacturing Engineering 31/2 (2008) 170-190.
75. W. Lengauer, K. Dreyer, Functionally graded hardmetals, Journal of Alloys and Compounds 338 (2002) 194-212.
76. K. Lukaszkowicz, L.A. Dobrzański, Structure and mechanical properties of gradient coatings deposited by PVD technology onto the X40CrMoV5-1 steel substrate, Journal of Materials Science 43/10 (2008) 3400-3407.

77. B. Major, T. Wierzchoń, E. Reinhold, W. Wołczyński, J. Bonarski, G. Krużel, Graded materials on titanium matrix, Material Engineering 6 (2000) 340-343.
78. G. Matula, Study on steel matrix composites with (Ti,Al)N gradient PVD coatings, Journal of Achievements in Materials and Manufacturing Engineering 34/1 (2009) 79-86.
79. FORSURF. Structural project in realisation, www.forsurf.pl, 2009-2012 (in Polish).
80. N. Gerdsri, R.S. Vatananan, S. Dansamasatid, Dealing with the dynamics of technology roadmapping implementation: A case study, Technical Forecasting & Social Change 76 (2009) 50-60.
81. Y. Yasunaga, M. Watanabe, M. Korenaga, Application of technology roadmaps to govermental innovation Policy for promoting technology convergence, Technical Forecasting & Social Change 76 (2009) 61-79.
82. R. Phaal, G. Muller, An architectural framework for roadmapping: Towards visual strategy, Technological Forecasting & Social Change 76 (2009) 39-49.